

STUDIES ON DIELECTRIC RESONATORS IN SUSPENDED SUBSTRATE
ENVIRONMENT FOR MILLIMETER WAVE APPLICATIONS

A Thesis Submitted
in Partial Fulfillment of the Requirement for the Degree of
Master of Technology

by
Rajiv Kumar Shukla

to the
Department of Electrical Engineering
INDIAN INSTITUTE OF TECHNOLOGY, KANPUR

February 1995

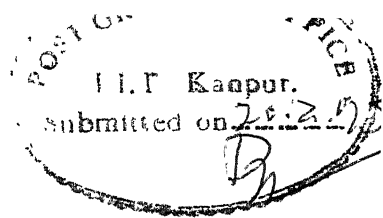
22 MAR 1985 / EE

CENTRAL LIBRA.
ANFUR

Acc. No. A. 119111

70
800.00
100.00

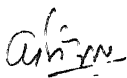
EE-1995-M-SHU-STU



Certificate

It is confirmed that the Analysis presented in this thesis entitled STUDIES ON DIELECTRIC RESONATORS IN SUSPENDED SUBSTRATE ENVIRONMENT FOR MILLIMETER WAVE APPLICATIONS, by Rajiv kumar shukla, has been carried out under my supervision and that this work has not been submitted elsewhere for a degree.

16th February 1995


(Dr. Animesh Biswas)
Asstt. Professor
Department of Electrical Engineering
I.I.T. Kanpur

Acknowledgements

My sincerest thanks goes to my research adviser Dr. Animesh Biswas, whose encouragement and assistance at various stages of this research work were most helpful. He sparkled many new, beautiful ideas in this work. It became a rewarding experience, to work under his able guidance and receiving a part of his tremendous knowledge.

I am indebted to Dr. N.C. Mathur, who generated a keen interest in electromagnetic and microwave field, by clearing all the doubts in a beautiful way. I will always remember him as an ideal educationist.

The inception of my research work is attributable to Dr. M. Sachidanand~~Q~~, who selected me for M.Tech. program. I profusely thank him for his kind support.

I extend my thanks to all my partners in EM discipline.

I am very grateful to my mother and my in laws for their support and encouragement during my studies.

I acknowledge the cheerful and worm company of Sanjeev, Mrs. and Mr. Atul my ever supporting neighbor, Maj. Arora, Roopam, Suman and many of those friends whose names are not mentioned here.

As a final personal note, I am grateful to my loving wife *Madhu* and my little baby *Ani* (Gillu) for their patience, love and encouragement during the time I devoted to my studies and research work

CONTENTS

1	INTRODUCTION	1
1.1	Dielectric Resonator : An Introduction	3
1.2	Methods of analysis	5
1.2.1	Approximate Methods	5
1.2.2	Rigorous Methods	6
1.3	Organization of the Thesis	8
2	CALCULATION OF RESONANT FREQUENCY USING EFFECTIVE DIELECTRIC CONSTANT TECHNIQUE	9
2.1	DWM method with EDC Approach	9
2.1.1	DWM Method	9
2.1.2	Use of EDC Approach	16
2.2	Numerical Implementation	18
2.3	Numerical Results	19
2.3.1	Comparison with Experimental Data	19
2.3.2	Comparison with DWM and Rigorous Methods	20
2.3.3	Effect of Design parameters on resonant frequency	20
3	ENERGY DISTRIBUTION OF DIELECTRIC RESONATOR IN SUSPENDED SUBSTRATE ENVIRONMENT	23
3.1	Electric energy distribution	23
3.1.1	Electrical Energy filling factor	25
3.2	Magnetic energy distribution	26
3.2.1	Magnetic Energy Filling Factor	29
4	COUPLING BETWEEN TWO SYMMETRICAL DIELECTRIC RESONATOR IN SUSPENDED SUBSTRATE	30
4.1	Direct coupled Cylindrical Resonators	30
4.1.1	Edge-coupled Resonators	33
4.1.2	Coupling between two DRs placed on Opposite sides of Suspended substrate	33
4.2	Numerical Results	34

5	COUPLING BETWEEN DIELECTRIC RESONATOR AND STRIP-CONDUCTOR WITH FINITE THICKNESS ON SUSPENDED SUBSTRATE	36
5.1	Methods of coupling in TE _{01δ} and TM _{01δ} modes	36
5.2	Coupling between DR and planner Transmission lines	37
5.3	Numerical Results	43
5.3.1	Comparison with Experimental Data	43
5.3.2	Coupling between Suspended stripline and DR	43
5.3.3	Coupling between Inverted Microstripline and a DR	43
6	CONCLUSION AND FUTURE DEVELOPMENTS	44
	APPENDICES	
	A Value Of Field Constants B_{1S}	46
	B Expressions for A_{ijS} and t_{sameS}	47
	B.1 A_{ij} Expressions	47
	B.2 t_{sameS} Expressions	48
	C Integrals involving Bessel Functions	49
	D Evaluation of volume integral $\iiint E \cdot J$	50
	D.1 Edge coupled DR	50
	D.2 Off layered coupling	51
	E Derivation of Integral $\int H \cdot ds$	52
	REFERENCES	54

LIST OF TABLES

1.1 Material properties of some DRs	5
2.1 Comparison of EDC method with Experimental Data[20]	19
2.2 Comparison of EDC and DWM methods with Rigorous methods	20
3.1 Electric Energy Filling Factor for various regions of resonant structure in suspended substrate Environment	26
3.2 Magnetic Energy Filling Factor for various regions of resonant structure in suspended substrate Environment	29

CHAPTER 1

INTRODUCTION

Reducing the cost of microwave circuits goes hand in hand with reducing their size. In this respect, microstrip line, stripline, and suspended stripline have been essential in eliminating bulky waveguides and rigid coaxial lines in a great majority of microwave systems. Only in a few and very demanding applications, such as high power transmission , or low-loss filtering, are waveguides still being used [7]. For realization of filters and oscillators, we need a frequency determining element which may be compatible with the microstripline, stripline or suspended stripline in size and with the conventional waveguide and coax resonators in performance, for miniaturization of microwave circuits. With the advent of high dielectric constant(ϵ_d) and high-Q dielectric resonators(DR) it is possible to meet above requirements and to provide an alternate solution for the conventional microwave resonators. Due to their wide variety of applications in microwave circuits, investigation of their circuit properties had been recognized as an important problem in early seventies[14-17]. These resonators offer various advantages in microwave field due to combination of properties they possess. Due to high dielectric constant, size of the dielectric resonator is smaller than the size of an empty cavity resonator operating at the same frequency, approximately by a factor of $1/\sqrt{\epsilon_d}$. They fill a gap between wave guide and planer transmission lines like microstripline, stripline, suspended stripline, or inverted microstripline by providing high-Q and temperature stability comparable to those of invar cavity resonators along with an integrability reaching to planer transmission line resonators. They offer versatility and are adoptable to various microwave structures and coupling configurations.

Numerous analysis and synthesis methods exist for studying the behavior of dielectric resonators. Dielectric waveguide model (DWM), Mode matching, Integral equation etc. are a few of them [7,14-18]. Recently, finite methods like finite element method and finite-difference time domain method, are also getting a great popularity with the availability of powerful computers[43].

In planer transmission lines , the microstripline has got a special importance for microwave integrated circuits, because of its compatibility and ease of manufacturing. But for higher frequencies especially in millimeter wave range(30-300 GHz), it faces the problems like higher losses, tight fabrication tolerances, handling fragility etc. and more seriously, it becomes very dispersive medium of transmission. The supplement to these problems are suspended stripline and inverted microstripline structures. These structures has lower losses, resulting in a higher Q-factor than microstripline because a greater portion of the field exists in the air than that in microstripline. In addition, a broader line width is possible for a prescribed characteristic impedance, and the TEM mode propagation is more pronounced, with less dispersion . Thus, numerical quasi-TEM analysis can be applied to yield sufficiently accurate results up to the millimeter wave frequency range[8]. Hence, these suspended substrate structures are very useful for millimeter wave applications.

Many references are available for getting the analysis of DR and the design parameters like resonant frequency[14-25], coupling coefficient between two DRs[29,30], and coupling between DR and microstripline[31,32,42] in MIC environment, that can be used for low microwave frequencies. But, not much information are reported about these parameters of a DR in *suspended-substrate environment*. A need for improved technique for providing design solution of DR in this environment has generated the keen interest to find out efficient and accurate design procedures.

This thesis studies the circuit properties of DR in suspended substrate environment, specially for millimeter wave applications. Emphasis is given on cylindrical DR operating in TE_{01d} mode, due to it's extensive use in microwave circuits and ease of exciting this mode. The main objective here is to develop suitable design criteria, so that dielectric resonators can be used as a circuit element in suspended substrate or MIC environment, to perform the prescribed operation as accurately as possible without resorting to the cut and try approach.

1.1 Dielectric Resonator : An Introduction

A dielectric resonator is made of a low loss, high dielectric constant, and temperature stable ceramic material in a regular geometric forms like pillbox, disc, tubular, spherical etc. (Fig. 1.1) [12,14]. For a practical resonator the cylindrical (disc type) structure is preferred over other type of structures because cylindrical resonators do not have a large number of degenerate modes and are easier to fabricate and mount in microwave circuits [43]. In this thesis cylindrical dielectric resonator have been dealt in detail, due to its simplicity and the above mentioned advantages. Application of spherical DR, for miniaturization of DR filter for mobile communication has also been reported, recently[38].

In 1939 R.D. Richtmayer observed that unmatelized dielectric objects can function as electric resonators. The first exploratory activities on dielectric resonators occurred in the 1960s with the analysis of resonant frequency and modes, studies of dielectric resonator(DR) and circuit properties, and other related topics about coupling with external circuits. At that time, DR had been used in paramagnetic spin resonance experiments, but the lack of suitable material precluded its practical applications in microwave components. These early studies however helped in the understanding of DRs and stimulated the efforts to

develop suitable dielectric materials having desired properties for use in microwave applications such as

- a. high dielectric constant ϵ_d
- b. high unloaded quality factor, Q_0
- c. low temperature coefficient of resonant frequency tf

The value of Q_0 limited by major imperfections of the conductor and the dielectric losses occurring inside the DR material. The conductor losses are incurred due to small but non zero conductivity of the dielectric material. The damping of oscillations of electrons caused by the alternating polarization of dielectric material exposed to the time harmonic electric field at microwave frequency, results in the dielectric losses. Typical values of Q_0 for a DR is $\sim 10,000$.

Temperature stability depends upon the effects of temperature on material and electrical properties of the resonator. These effects include the change in dimensions of the DR and the variation of dielectric constant ϵ_d . The resonant frequency of a DR mainly depends upon its dimensions and dielectric constant. These result in the deviation of the resonant frequency with temperature change. The sensitivity of resonant frequency with temperature is denoted by tf , which is also known as temperature coefficient of the resonant frequency.

Various new compositions having acceptable values of the ϵ_d , tf , and Q_0 were explored with the advancement in material technology. These include ceramic mixtures containing TiO_2 , various titanates, zirconates and glass ceramic mixtures [12,13]. Temperature compensated composite structure resonators using ferrite and ferroelectrics were also reported. This rapid development in material technology removed the restriction on the frequency range of the DR,

and now they can even be applied to microwave circuits operating in millimeter wave frequency range[13,35]. Table 1.1 lists some important properties of commonly used materials for DR.

Table 1.1: Material properties of some DRs [7,12]

Material composition	Q_0	ϵ_d	Frequency range (GHz)	Temperature coefficient τ_f (ppm/ $^{\circ}$ C)
(ZrSn)Ti Oxide	>10,000 (4.5 GHz)	35.7- 36.4	1.45-8.86	-3 to +9
BaLnTi Oxide	>3,000 (3.0 GHz)	80.0	0.7-3.62	-3 to +9
BaZnTaTi Oxide	>10,000 (10.0GHz)	27.6- 30.6	5.5 - 32.2	-4 to +4
Ba Titanium Oxide	>6,000 (4.5GHz)	36.6- 38.3	0.8-5.21	0 to 4

1.2 Methods of analysis

After availability of dielectric resonator with excellent properties, researchers started investigating the fields and the resonant frequency of DR in different circuit environments, using various approximate and rigorous analysis methods.

1.2.1 Approximate Methods

An accurate mathematical description of the electromagnetic field in a dielectric resonator is considerably more complicated than the field distribution in a hollow metallic waveguide resonator. Approximate methods treated DR as the dual of a metallic cavity. DR was modeled as a section of dielectric rod waveguide [14]. This model was simplified by introducing some approximation such as by assuming perfect magnetic conductor (PMC) wall over the curved surface of the DR. Cohn's method falls in the same class[14]. He modeled a cylindrical DR as a section of

cylindrical dielectric waveguide with air dielectric boundary in z (axial) direction (Fig. 1.2), then calculated resonance frequency and the coupling coefficient. The air filled sections on both sides of DR remain below cutoff due to low dielectric constant than that in the dielectric region. Thus the modes in the air filled regions are evanescent and fields decay exponentially in the axial direction away from each air-dielectric boundary. This model gives an error of more than 6% in resonant frequency calculation, but it helped in designing waveguide dielectric resonator filter. This model does not take into account of the field leaking through this surface, because it puts a fictitious open circuit (i.e. PMC) over the cylindrical surface of the DR. In an actual DR magnetic field is always present in the vicinity of the cylindrical surface containing the circumference of the DR due to air-dielectric boundary. Outside of the resonator magnetic field decays very rapidly with distance. A more accurate method, based on the variational procedure for computing the resonant frequency in $TE_{01\delta}$ mode was later reported by Konishi et al.[16]. Iveland [15] computed resonant frequency for a square pillbox shape dielectric resonator using a similar procedure. A more realistic model for a DR placed under shielded condition was used by Itoh and Rudokos[17]. They made this model more realistic by removing the assumption of PMC of the Cohn's model and took into account the field distribution outside the resonator also. Even this method gives resonant frequency which is high by about 5% for isolated resonators. However, due to its simplicity in calculation it was adopted by many researchers.

1.2.2 Rigorous Methods

The approximate methods, described in the last section, are useful as aids in understanding the principles of operation of DRs, and they may be helpful to the initial stages of the analysis or design process, but, they fail to

provide the high accuracy usually required in present-day microwave circuit design. In an attempt to obtain accurate solution of the problem, DR placed in MIC environment was analyzed using rigorous analysis methods. Mode matching technique is used in some of these methods like Radial mode matching method and Axial mode matching method. Zaki and Chen[37] have applied the axial mode matching method to determine the TE, TM and hybrid modes of a DR placed symmetrically in a cylindrical cavity. Tsuji et al.[25] analyzed an isolated DR by expanding the fields inside and outside a pillbox resonator in terms of spherical wave functions and by matching the tangential field components of the two regions at the resonator's surface. Van Bladel applied perturbational approach by expanding the fields in asymptotic series in inverse power of the $\sqrt{\epsilon_d}$. This method is exact only in the limit as ϵ_d goes to infinite. Glisson et al.[24] used integral equation method by choosing a suitable Green's function which also constitute the kernel of the integral equation. The success of this method depends upon the choice of the Green's function which is simpler in the case of an isolated dielectric resonator where free-space Green's function is required. In case of shielded resonators, the determination of the Green's function is more difficult, particularly for more complex resonators. Glisson simplified this task by subdividing the resonator into two regular partial regions and by erecting a electric or magnetic wall at boundary between the regions. For maintaining the correct field in both regions magnetic or electric current sheets were postulated on this wall. By enforcing the continuity conditions between the partial regions, an integral equation was obtained, which was solved using method of moments. The zeros of the resultant matrix determinant was calculated to obtain the resonant frequency.

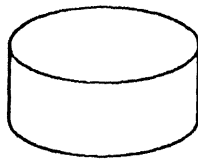
All these rigorous analytical methods are versatile and allow a more general range of applications. However, these methods are not used in practical design, because they are quite complicated as well computationally intensive. A

method which offers both simplicity and accuracy is required for computer aided design purpose. A method using effective dielectric constant (EDC) technique with DWM method is suggested by Mongia [20] for cylindrical DR. This method is easy to implement and gives results, which are accurate to 1% .

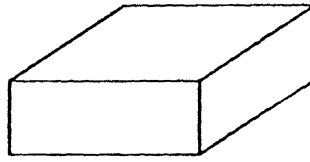
1.3 Organization of the Thesis

Design of microwave circuits employing dielectric resonator, like filters, oscillators, radar detectors, speed guns, cellular telephones etc., requires an accurate knowledge of resonant frequency of DR and its energy distribution in all the regions of the environment and its coupling with other circuit elements (transmission lines, other resonators etc.). In this thesis these design aspects have been studied for a cylindrical dielectric resonator placed in Suspended-substrate environment. Stress is over dominant $TE_{01\delta}$ mode of the resonator.

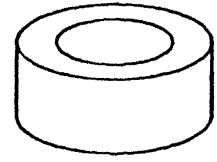
The thesis is divided into five chapters. Chapter 2 discusses the use of EDC method combined with DWM method for calculating resonant frequency and field distribution of a cylindrical resonator for $TE_{01\delta}$ mode. Chapter 3 presents the electrical and magnetic energies distribution in all the regions of the DR's environment. In chapter 4 coupling between two identical dielectric resonators is presented for three very important configurations, along with the evaluation of coupling coefficient between them. And the last chapter deals with the characterization of coupling between cylindrical resonator and two very important transmission line configurations like suspended stripline and inverted microstripline with finite thickness conductor. Following this chapter comes the conclusion and future scope these studies.



(a) Cylindrical



(b) Rectangular box



(c) Hollow cylinder

Fig 1.1: Dielectric resonators in different geometrical shapes

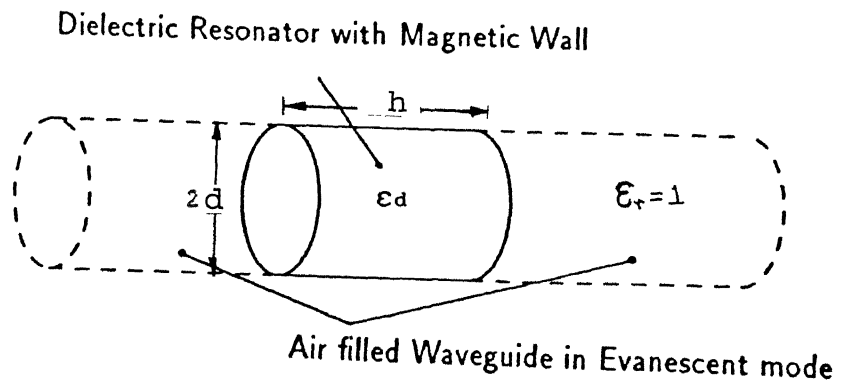


Fig 1.2: Dielectric resonator as a section of Dielectric rod (Chon's model) [14]

Chapter 2

CALCULATION OF RESONANT FREQUENCY USING EFFECTIVE DIELECTRIC CONSTANT TECHNIQUE

In the design of microwave circuits having DR, the first step is the analysis for finding the field distribution and resonant frequency of the dielectric resonator(DR). This analysis forms the subject matter of the present chapter.

Initially, the researchers tackled this problem by the approximate methods such as second order magnetic wall model[14] for finding simple design solutions for the lower order modes. Though approximate models are very efficient yet they are not accurate enough. This deficiency can be overcome by rigorous methods such as Method of moments and Green's function approach, but, at the price of increased complexity and computational time. Researchers are always in search of an efficient method capable of producing results comparable in accuracy to those obtained from rigorous methods, for most frequently used $TE_{01\delta}$ mode.

To analyze the dielectric resonator in $TE_{01\delta}$ mode, the use of Effective Dielectric Constant (EDC) technique applied with Dielectric Waveguide Model (DWM) method, is described in this chapter

2.1 DWM method with EDC Approach

2.1.1 DWM Method

In DWM method a dielectric resonator is considered as the dual of a metallic cavity. Our Dielectric waveguide model method is similar to Itoh's method [17] except in field expressions selected for axial magnetic field (Hz). The dielectric rod waveguide when truncated becomes a dielectric resonator, in same way as a truncated hollow waveguide

becomes a resonant cavity. For circular symmetric field configurations (lower frequency modes), suitable field expressions can be found for axial field components (E_z and H_z) from the knowledge of field analysis for dielectric rod waveguide. When we apply the proper boundary conditions these field expressions give characteristic equation, the solution of which gives the resonant frequency. Analysis presented below is for $TE_{01\delta}$ mode but it equally applies to $TM_{01\delta}$ mode by virtue of the principle of duality.

Maxwell's equations for TE_{0n} case

For a source free, isotropic and homogeneous medium, the fundamental Maxwell's equations can be written as follows:

$$\nabla \times \underline{E} = -j\omega\mu\underline{H}$$

$$\nabla \times \underline{H} = j\omega\varepsilon\underline{E} \quad (2.1)$$

and,

$$\nabla \cdot \underline{E} = 0$$

$$\nabla \cdot \underline{H} = 0 \quad (2.2)$$

Combination of above two equations gives us well known vector Helmholtz's equations given below :

$$\nabla^2 \underline{E} + k^2 \underline{E} = 0$$

$$\nabla^2 \underline{H} + k^2 \underline{H} = 0 \quad (2.3)$$

where k is called the wave number of the medium and in general it is a complex quantity. For a dielectric medium of relative dielectric constant ε_r , the wave number k is given by:

$$k^2 = k_0^2 \varepsilon_r \quad (2.4)$$

where, $k_0 = 2\pi f_0 \sqrt{\mu_0 \epsilon_0}$ and f_0 is resonant frequency.

To obtain the fields in all the regions of a structure, it is convenient to start from the axial component of the electric or magnetic field. Other field components can be obtained from this axial field with the help of Maxwell's equations.

For TE^z mode (i.e. $E_z = 0$), We can start from the axial magnetic field i.e. H_z . Then vector Helmholtz's equation (2.3), reduces to scalar form as follows:

$$\nabla^2 H_z + k^2 H_z = 0 \quad (2.5)$$

we can solve this equation by well known method of separation of variables. The field components for TE^z circular symmetrical case ($\partial/\partial z = 0$) are expressed as:

$$E_r = 0 \quad H_r = -\frac{\partial^2 H_z}{\nu^2 \partial z \partial r}$$

$$E_\phi = -\frac{j\omega\mu}{\nu^2} \frac{\partial H_z}{\partial r} \quad H_\phi = 0$$

$$E_z = 0 \quad H_z = H_0 \sin \nu r \quad (2.6)$$

Here, ν is defined as the radial wave number, and in general is given by :

$$\nu^2 = \pm(k^2 - k_z^2); \text{ where } k_z \text{ is the axial wave number.} \quad (2.7)$$

Field distributions in the resonator

The cross-sectional view of cylindrical resonator placed in suspended substrate environment is shown in Fig. 2.1. The resonator material is assumed to be a perfect dielectric characterized by the real scalar relative permittivity ϵ_r and the real scalar permeability μ ($=\mu_0$). To simplify the analysis, this composite structure is divided into eight regions with a different set of field components. Here, the

proper choice of H_z in different regions depends on the requirements imposed by physical geometry and the analyticity of the field at the origin. It also should satisfy the wave equation (2.5).

Inside the resonator, H_z should represent standing wave in z direction and wave number $\nu = k_r$ should be real to fulfill the requirement of DR as a energy storing element. The solution of eqs.(2.5) in cylindrical coordinates, using method of separation of variables with above mentioned conditions gives the following form of expressions for H_z in region no.1

$$H_{z1} = \{\cos(\beta_1 z) + B_1 \sin(\beta_1 z)\} J_0(k_r r) \quad (2.8)$$

where J_0 is the Bessel function of the first kind and zero order and k_r is related to β_1 by separation relation

$$k_r^2 + \beta_1^2 = \epsilon_d k_0^2 \quad (2.9)$$

Outside the resonator, H_z should be axially symmetric. but, decaying in nature in the direction away from the resonator for confirming the maximum energy storage inside the resonator. This decay in radial direction can be represented by modified bessel function, so, outside the resonator (in the radial direction) radial wave number becomes imaginary. Finally, normal magnetic field H_z should vanish at metallic surfaces. Again solving eqs(2.5) with these conditions, H_z in the rest of the regions (2,3,4,5,6,7 and 8) can be written as :

$$H_{z2} = B_2 \cdot \exp(-\alpha_d d_1) \cdot \sinh\{\alpha_a (d_1 - z)\} J_0(k_r r)$$

$$H_{z3} = B_3 \cdot \{\cos(\beta_2 z) + B_4 \cdot \sin(\beta_2 z)\} J_0(k_r r)$$

$$H_{z4} = B_5 \cdot \exp(-\alpha_s d_2) \cdot \sinh\{\alpha_s (d_2 + z)\} J_0(k_r r)$$

$$H_{z5} = B_6 \cdot \exp(-\alpha_d d_1) \cdot \sinh\{\alpha_a (d_1 - z)\} K_0(k_a r)$$

$$H_{z6} = B_7 \{ \cos(\beta_1 z) + B_1 \sin(\beta_1 z) \} K_0(k_a r)$$

$$H_{z7} = B_8 \{ \cos(\beta_2 z) + B_4 \sin(\beta_2 z) \} K_0(k_a r)$$

$$H_{z8} = B_9 \exp(-\alpha_s d_2) \sinh\{\alpha_s (d_2 + z)\} K_0(k_a r) \quad (2.10)$$

where K_0 is the modified Bessel function of the second kind and zero order, and separation relations in these regions are

$$k_a^2 = \beta_1^2 - k_o^2 \quad (2.11)$$

$$k_a^2 = \beta_2^2 - \epsilon_{s1} k_o^2 \quad (2.12)$$

$$k_r^2 - \alpha_a^2 = k_o^2 \quad (2.13)$$

$$k_r^2 - \alpha_s^2 = \epsilon_{s2} k_o^2 \quad (2.14)$$

The transverse field components in various regions are found by substituting (2.8) and (2.10) into (2.6), and are given as

Region 1

$$E_{\phi 1} = - \frac{j\omega\mu_o}{k_r} \{ \cos(\beta_1 z) + B_1 \sin(\beta_1 z) \} J_1(k_r r)$$

$$H_{r1} = (\beta_1 / k_r) \{ \sin(\beta_1 z) - B_1 \cos(\beta_1 z) \} J_1(k_r r) \quad (2.15)$$

Region 2

$$E_{\phi 2} = - \frac{j\omega\mu_o}{k_r} B_2 \exp(-\alpha_a d_1) \sinh\{\alpha_a (d_1 - z)\} J_1(k_r r)$$

$$H_{r2} = B_2 (\alpha_a / k_r) \exp(-\alpha_a d_1) \cosh\{\alpha_a (d_1 - z)\} J_1(k_r r)$$

$$(2.16)$$

(

Region 3

$$E\phi_3 = - \frac{j\omega\mu_0}{k_r} B_3 \{ \cos(\beta_2 z) + B_4 \sin(\beta_2 z) \} J_1(k_r r)$$

$$H_{r3} = B_3 \cdot (\beta_2 / k_r) \cdot \{ \sin(\beta_2 z) - B_4 \cos(\beta_2 z) \} J_1(k_r r) \quad (2.17)$$

Region 4

$$E\phi_4 = - \frac{j\omega\mu_0}{k_r} B_5 \exp(-\alpha_s d_2) \sinh\{\alpha_s (d_2 + z)\} J_1(k_r r)$$

$$H_{r4} = -B_5 \cdot (\alpha_s / k_r) \cdot \exp(-\alpha_s d_2) \cosh\{\alpha_s (d_2 + z)\} J_1(k_r r) \quad (2.18)$$

Region 5

$$E\phi_5 = \frac{j\omega\mu_0}{k_a} B_6 \exp(-\alpha_a d_1) \sinh\{\alpha_a (d_1 - z)\} K_1(k_a r)$$

$$H_{r5} = -B_6 \cdot (\alpha_a / k_a) \cdot \exp(-\alpha_a d_1) \cosh\{\alpha_a (d_1 - z)\} K_1(k_a r) \quad (2.19)$$

Region 6

$$E\phi_6 = \frac{j\omega\mu_0}{k_a} B_7 \{ \cos(\beta_1 z) + B_1 \sin(\beta_1 z) \} K_1(k_a r)$$

$$H_{r6} = -B_7 \cdot (\beta_1 / k_a) \cdot \{ \sin(\beta_1 z) - B_1 \cos(\beta_1 z) \} K_1(k_a r) \quad (2.20)$$

Region 7

$$E\phi_7 = \frac{j\omega\mu_0}{k_a} B_8 \{ \cos(\beta_2 z) + B_4 \sin(\beta_2 z) \} K_1(k_a r)$$

$$H_{r7} = -B_8 \cdot (\beta_2 / k_a) \cdot \{ \sin(\beta_2 z) - B_4 \cos(\beta_2 z) \} K_1(k_a r) \quad (2.21)$$

Region 8

$$E\phi_8 = \frac{j\omega\mu_0}{k_a} B_9 \exp(-\alpha_s d_2) \sinh\{\alpha_s (d_2 + z)\} K_1(k_a r)$$

$$H_{r8} = B_9 \cdot (\alpha_s / k_a) \cdot \exp(-\alpha_s d_2) \cosh\{\alpha_s (d_2 + z)\} K_1(k_a r) \quad (2.22)$$

The value of unknown coefficients B_i s, can be evaluated by applying the boundary conditions at the interfaces of two regions, and are given in appendix A.

Resonant frequency f_0

If k_r and β_1 are known the resonant frequency f_0 can be calculated from eqs. (2.9). The concept of dielectric waveguide model (DWM) is used for determination of k_r and β_1 [20]. The k_r and β_1 are determined as follows.

Determination of k_r

The resonator is first assumed to extend to infinity in z direction (Fig. 2.2(a)) for determining k_r . We assume that this infinite dielectric cylinder carries TE_{01} as the propagating mode, and that k_r is the radial wave number for this cylinder for $r < d$. Applying the continuity condition for tangential electric field and normal magnetic field components at the boundaries of region 1, gives following characteristic equation:

$$\frac{J_1(k_r d)}{k_r J_0(k_r d)} + \frac{K_1(k_a d)}{k_a K_0(k_a d)} = 0 \quad (2.23)$$

Radial wave number k_r is related to k_a by

$$k_a = \{(\epsilon_d - 1.0)k_0^2 - k_r^2\}^{1/2} \quad (2.24)$$

k_r and k_a can be computed by solving Eqs.(2.23) and (2.24).

Determination of β_1

The structure of Fig. 2.2 is assumed to be a radial triple slab guide (Fig. 2.2(b)), along which the TE_{01} guide mode is propagating. In other words it is assumed that the axial wave number β_1 is the same as that of a triple layer slab guide structure, obtained by extending the resonator to infinity in the radial direction. When we apply the boundary conditions at the interfaces of these regions we get one more transcendental equation, given by

$$\beta_2 [M_2 \{ \tan(\beta_2 h/2) - \tan(\beta_2 d_3) \} + \tan(\beta_2 h/2) \cdot \tan(\beta_2 d_3) + 1.0]$$

$$[M_2 + \tan(\beta_2 d_3) - \tan(\beta_2 h/2) + M_2 \tan(\beta_2 h/2) \tan(\beta_2 d_3)]$$

$$- \frac{\beta_1 [\tan^2(\beta_1 h/2) + 2 M_1 \tan(\beta_1 h/2) - 1.0]}{[M_1 - M_1 \tan^2(\beta_1 h/2) + 2.0 \tan(\beta_1 h/2)]} = 0 \quad (2.25)$$

where,

$$M_1 = (\beta_1 / \alpha_a) \cdot \tanh(\alpha_a h_a); \text{ and}$$

$$M_2 = (\beta_2 / \alpha_s) \cdot \tanh(\alpha_s h_{s2}) \quad (2.26)$$

We get the value of k_r by solving transcendental equation (2.23) in conjunction with equation (2.24). Then we can solve the equation (2.25) for the height of the DR for specified resonant frequency f_0 , after substituting the values of $\beta_1, \beta_2, \alpha_a$, and α_s from separation relations (2.12) - (2.14).

For given dimensions of the DR, the resonant frequency of the DR is obtained by satisfying two transcendental equations (2.23) and (2.25) simultaneously, for suspended substrate as well as microstrip ($\epsilon_{s1} = \epsilon_{s2} = \epsilon_s$) environment.

2.1.2 Use of EDC Approach

The DWM method gives higher value of the resonant frequency f_0 . In higher frequency range specially for millimeter waves this error is very large. Recently Mongia [20] suggested Effective Dielectric Constant (EDC) approach for calculating radial wave number k_r , which greatly enhances the accuracy of DWM method. According to this approach radial wave number k_r is assumed to be the wave number of an infinitely long cylindrical waveguide having the same radius as that of the DR, but having a dielectric constant ϵ_{eff} which is less than that of the resonator. In this method k_r and k_a are related

by

$$k_a = \{ (\epsilon_{eff} - 1.0) k_o^2 - k_r^2 \}^{1/2} \quad (2.27)$$

An approximate expressions for ϵ_{eff} [20] is given as follows

$$\epsilon_{eff} = (\epsilon_{eff}^a + \epsilon_{eff}^b) / 2 \quad (2.28)$$

where

$$\begin{aligned} \epsilon_{eff}^a &= \epsilon_d - (\epsilon_d - \epsilon_{eff}^o) \cdot (h_{s1} + h_{s2}) / d \text{ if } (h_{s1} + h_{s2}) < d \\ &= \epsilon_{eff}^o \text{ otherwise} \end{aligned} \quad (2.29)$$

$$\begin{aligned} \epsilon_{eff}^b &= \epsilon_d - (\epsilon_d - \epsilon_{eff}^o) \cdot h_a / d \text{ if } h_a < d \\ &= \epsilon_{eff}^o \text{ otherwise} \end{aligned} \quad (2.30)$$

ϵ_{eff}^o is obtained by

$$\epsilon_{eff}^o = \frac{k_r^2(\epsilon_d)}{k_o^2} \quad (2.31)$$

Here, $k_r(\epsilon_d)$ is the same radial wave number given in eqs (2.24).

Thus the values of k_r , and k_a are modified by EDC method and also, the values of other eigen values are correspondingly modified. When $(h_{s1} + h_{s2}) = h_a = 0$, the value of ϵ_{eff} reduces to ϵ_d and this method gives the exact value of resonant frequency for a dielectric post resonator. When $(h_{s1} + h_{s2})$ and h_a both tends to infinity with $\epsilon_{s1} = \epsilon_{s2} = 1.0$, ϵ_{eff} reduces to $k_r^2(\epsilon_d) / k_o^2$, and gives the expression for an isolated resonator.

Results obtained by EDC approach are comparable to those obtained by rigorous methods.

2.2 Numerical Implementation

Above analysis is very general in nature, that is applicable for suspended substrate environment as well as for MIC environment (By putting $\epsilon_{s1} = \epsilon_{s2} = \epsilon_s$ and $h_{s1} = h_{s2} = h_s/2$). Based on this analysis software programs for both, pure DWM and DWM with EDC approach, named f-DWM.f and f-EDC.f, are developed for the calculation of the resonant frequency for a given dimensions of the DR, and the supporting structure.

In these programs computation is started with finding the roots of equation (2.23) using Newton-Raphson method with following initial approximate value for $k_r(\epsilon_d)$:

$$k_r(\epsilon_d) = [0.951 X_{01} + 0.222\{(\epsilon_d - 1)(k_0 d)^2 - 0.951 X_{01}^2\}^{1/2}] / d \quad (2.32)$$

where $X_{01} = 2.405$, and is the first root of the equation $J_0(x) = 0$. However calculation of k_r in above closed form expression requires the value of f_0 also. A wise guess for this value reduces the number of iterations required for convergence of the solution of the equation (2.23) and consequently the computational time of the programs. This value is obtained from following empirical relation, obtained by curve fitting process

$$f_0(\text{GHz}) = 36.0 \left(\frac{1}{h} + \frac{e^{-h_a}}{15.0} + \frac{3.75}{d} \right) / \sqrt{\epsilon_d} \quad (2.33)$$

here h is height in mm, d is radius in mm, and ϵ_d is dielectric constant of the DR. And h_a is the distance in mm of the top conductor wall from the top of the DR. This relation gives the starting value of f_0 accurate to $\pm 4\%$.

Other eigen values and the height of the resonator can be computed, when k_r and k_a are determined. Repeated iterative procedure is used to get the value of f_0 within

tolerable accuracy.

2.3 Numerical Results

2.3.1 Comparison with Experimental Data

The results obtained for f_0 of a DR from above programs are presented in Table 2.1 along with the experimental results [20] in MIC environment, because of non availability of experimental data in the literature for suspended-substrate environment. But, as mentioned earlier, it is a general analysis which is applicable for both types of the environment, so the verification in either case with experimental results validate the analysis.

A comparison of theoretical and experimental results shows a good agreement in all cases. the difference between the two results is less than 1% in most cases.

Table 2.1: Comparison of EDC method with Experimental Data[20] ($d = 4.55$ mm, $\epsilon_d = 37.1$, $h_a \rightarrow$ infinite)

h_{s1} $=h_{s2}$ $=h_s/2$ (mm)	ϵ_{s1} $=\epsilon_{s2}$ $=\epsilon_{rs}$	Resonant frequency f_0 (GHz)					
		$h = 2.0\text{mm}$		$h = 4.04\text{mm}$		$h = 6.96\text{mm}$	
		Exp.	Theory	Exp.	Theory	Exp.	Theory
0.19	2.22	8.81	8.89	6.46	6.46	5.43	5.37
0.4	2.22	8.3	8.26	6.3	6.24	5.34	5.28
1.19	2.22	7.39	7.44	5.91	5.87	5.17	5.09
1.58	2.22	7.3	7.3	5.82	5.79	5.14	5.05
0.32	9.6	8.4	8.43	6.31	6.31	5.37	5.31

Table 2.2 Comparison of EDC and DWM methods with Rigorous methods

Structural parameters						Resonant frequency (GHz)		
ϵ_d	$\epsilon_{s1} = \epsilon_{s2}$	d (mm)	h (mm)	$h_{s1} = h_{s2}$ (mm)	h_a (mm)	Rigorous methods	EDC tech	pure DWM method
38.0	1.0	2.86	2.38	0.36	inf.	9.83	9.82	10.22
38.0	1.0	2.86	2.38	1.43	inf.	9.16	9.14	9.85
35.2	9.6	2.43	1.81	0.32	inf.	12.4	12.37	12.87
34.19	9.6	7.49	7.48	0.35	0.72	4.35	4.33	4.35
34.21	9.6	7.00	6.95	0.35	1.25	4.52	4.50	4.53
36.2	1.0	2.03	5.15	1.465	2.93	10.50	10.36	10.85
36.2	1.0	4.00	2.14	2.215	4.43	7.76	7.68	8.365

2.3.2 Comparison with DWM and Rigorous Methods

Using this EDC method the results were computed for microstripline configuration, and the results are compared with approximate [17] and rigorous methods available in the standard literature. Table 2.2 shows this comparison. It is to be noted that the present technique gives results having an accuracy comparable to that of rigorous methods. The difference never exceeds more than 1%. In Fig. 2.3, results obtained using pure DWM method are also compared. It is seen that when h_a is small as compared to d then the error of the DWM method in calculating f_0 is very small. This is expected since ϵ_{eff} for this case almost reduces to ϵ_d .

2.3.3 Effect of Design parameters on f_0

Various electrical and physical parameters of the circuit, which are under the control of the designer at time of the fabrication the circuit, may change the resonant frequency of DR in the circuit. . Information presented in Figs. 2.4

to 2.6 shows the impact of these control variables over resonant frequency f_0 .

Fig. 2.4 shows the effect of separation (h_a) between top conductor plate and the top surface of the DR, over f_0 . Variation of resonant frequency with changing h_a can be explained by the cavity perturbation theory. When a metal wall of a resonant cavity is moved inwards, the resonant frequency of the cavity will decrease if the stored energy of the displaced field is predominantly electric. Otherwise, when the stored energy close to metal wall is magnetic, as in the case of shielded $TE_{01\delta}$ mode, the f_0 will increase [7]. Fig. 2.5 is showing the effect of the dielectric constant (ϵ_d) of DR, on its resonant frequency. We find that the resonant frequency decreases with increase in the value of ϵ_d . Hence the material of DR should be temperature stable to get frequency stability. Fig. 2.6 shows the variation of f_0 with substrate thickness (h_{s1}) for different values of substrate dielectric constant (ϵ_{s1}).

Resonator Tuning :

Tuning a dielectric resonator means adjusting its resonant frequency by mechanical or electrical means. Several techniques can be used to achieve this like

- # changing the thickness of the dielectric resonator.

- # perturbing the fringing fields outside the DR via screws, tuning stubs, or ferromagnetic material, etc.

- # perturbing the DR's f_0 by the so-called double resonator configuration, where two halves of the DR act as one. A tuning range (up to 20%) can be achieved with little degradation in Q factor by this method.

- # Optical tuning, magnetic tuning and electric tuning is also used.

The choice of a tuning method requires the consideration of the following factors:

- a. the mode to be tuned,

- b. the mechanical configuration of the final device, and

c. the tuning range desired and its direction(lower or higher frequencies)

For example, the tuning of TE modes is easily achieved by metallic or dielectric tuning stubs placed perpendicular to the dielectric resonator's top surface. Fig. 2.7 shows a schematic of the general effect of these methods. Metal tuning stubs (a) moving towards the DR will pull the frequency up and dielectric tuning stubs (b) will push the frequency down.

Approximately 20% of f_0 tuning can be achieved by these methods. It is, however, good practice to restrict this amount to below 5% to minimize degradation of both temperature coefficient and unloaded Q.

(Numbers inside circles shows the Region No.)

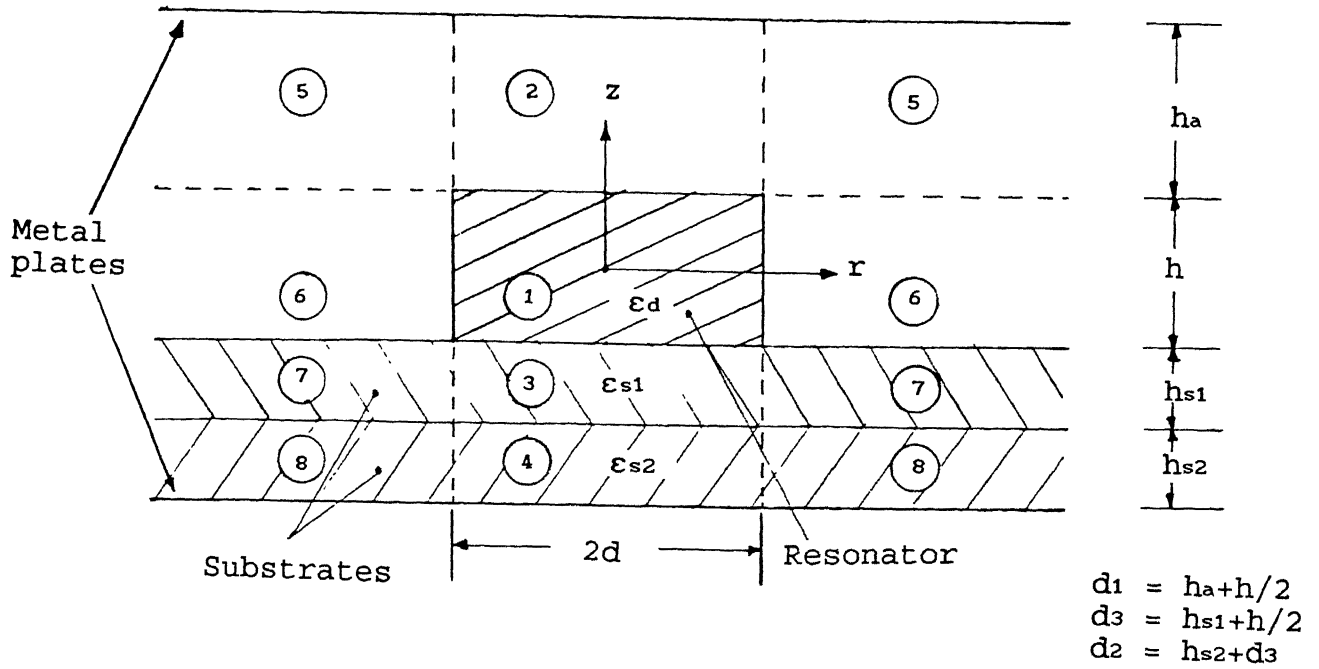


Fig. 2.1: Cylindrical dielectric resonator in suspended substrate environment

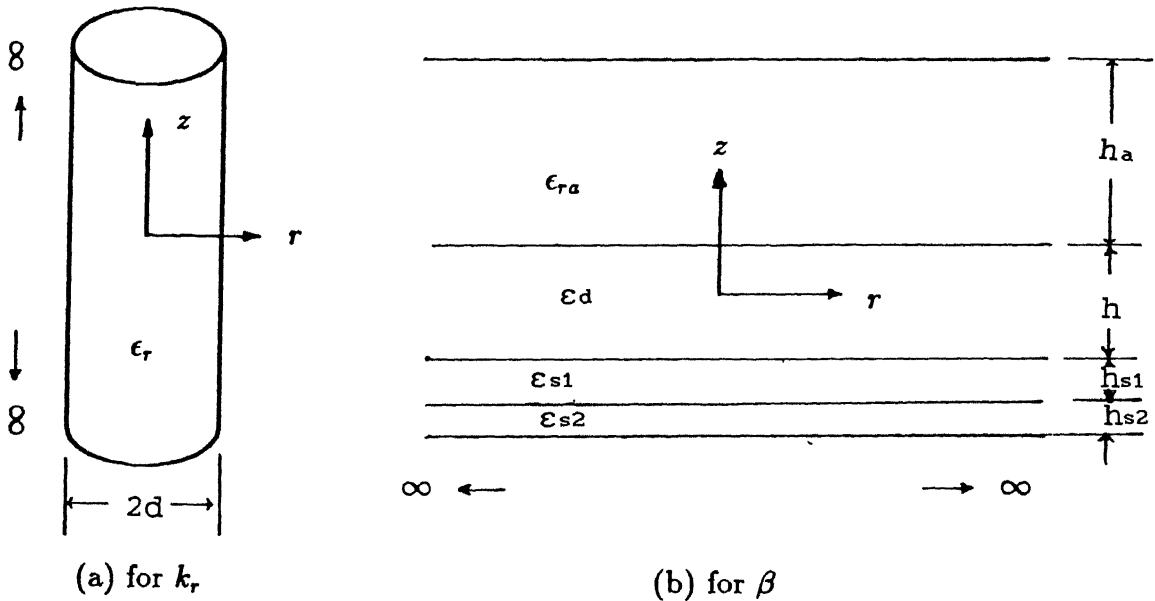


Fig. 2.2: Determination of k_r and β_1 [20]

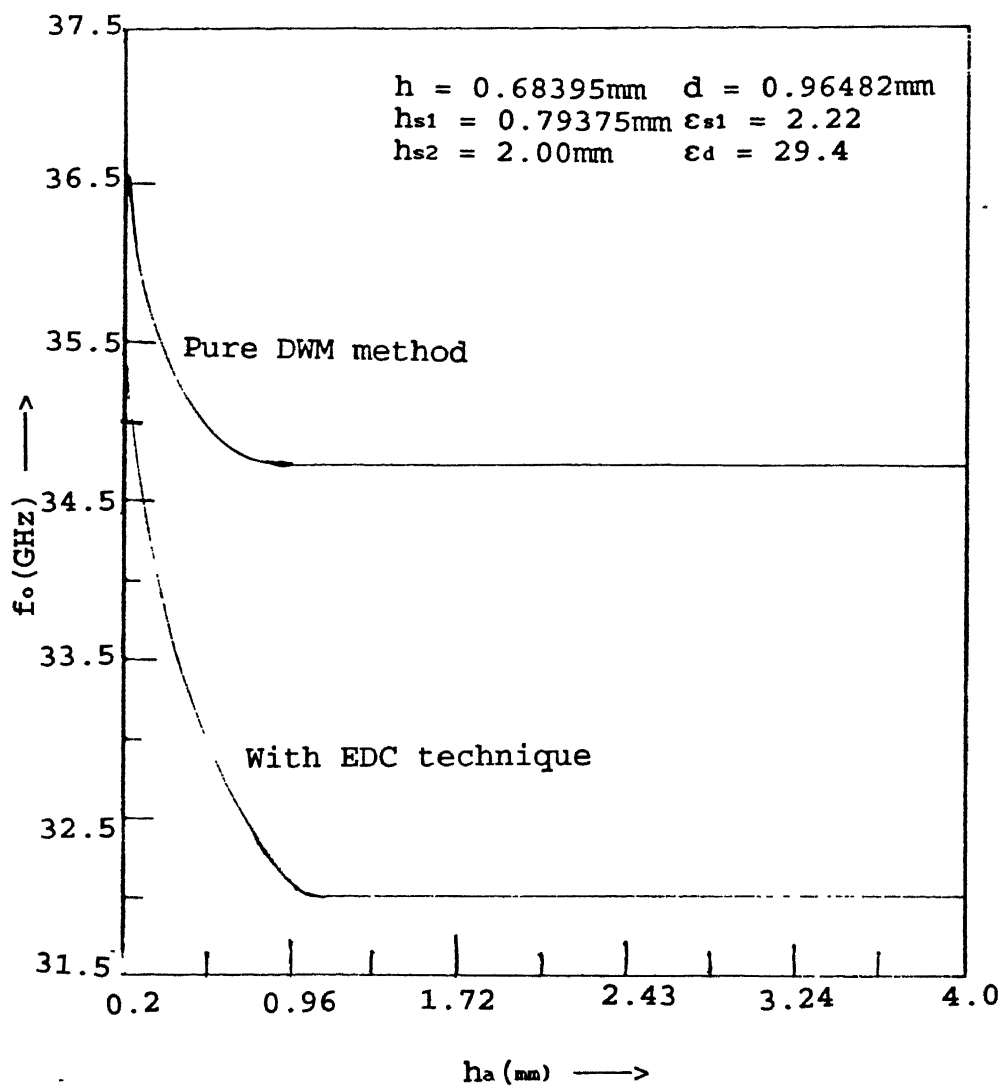


Fig. 2.3: Comparison of EDC technique and pure DWM method

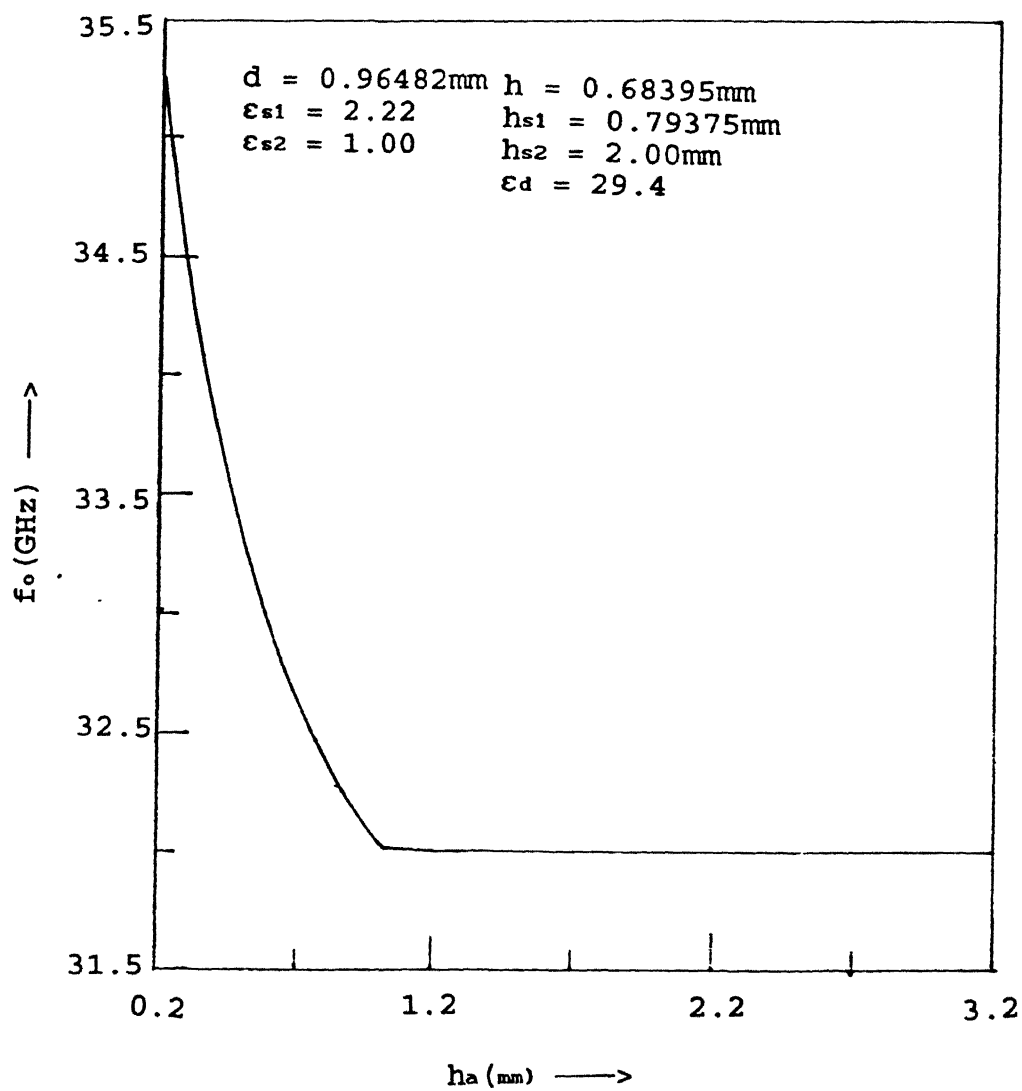


Fig. 2.4: Effect of changing height of top conductor wall (h_a) on resonant frequency f_o .

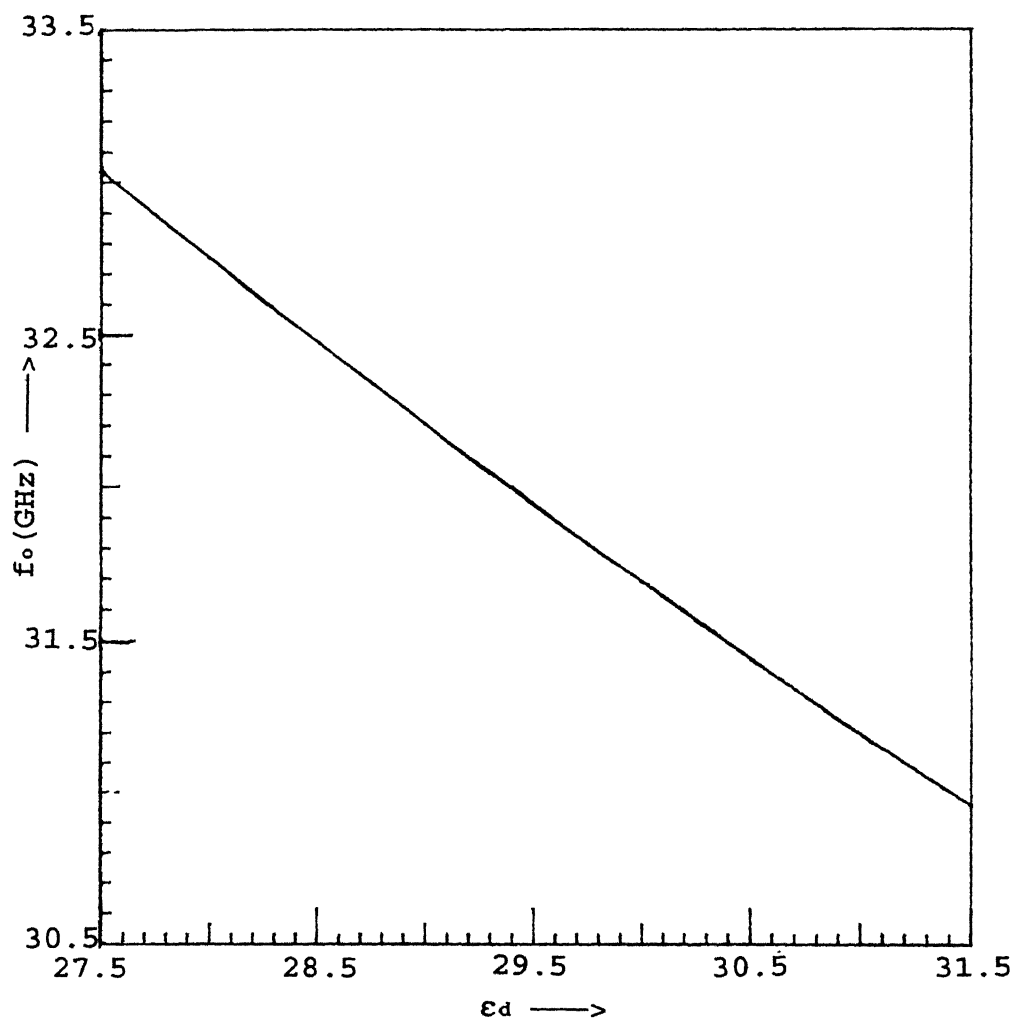


Fig. 2.5: Effect of changing dielectric constant (ϵ_d), of DR on resonant frequency f_0 .

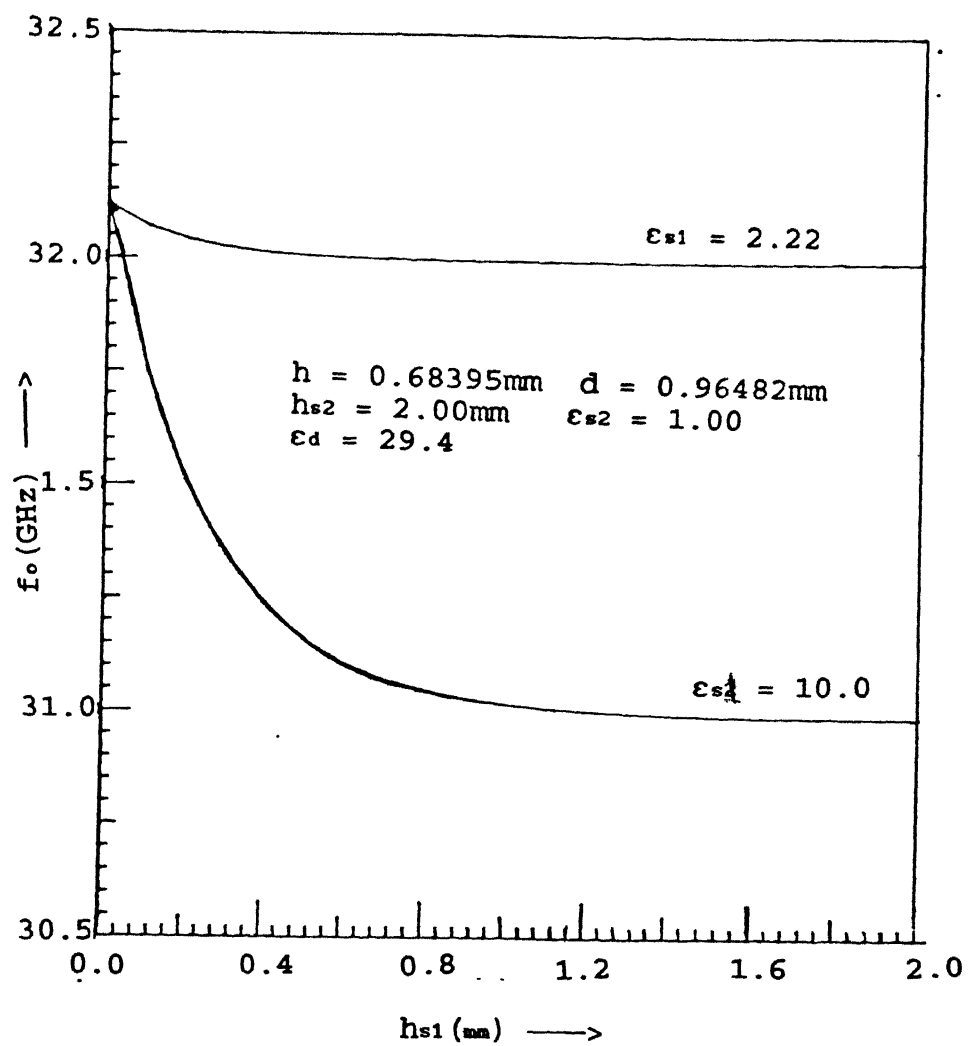


Fig. 2.6: Effect of changing thickness and dielectric constant of the suspended substrate.

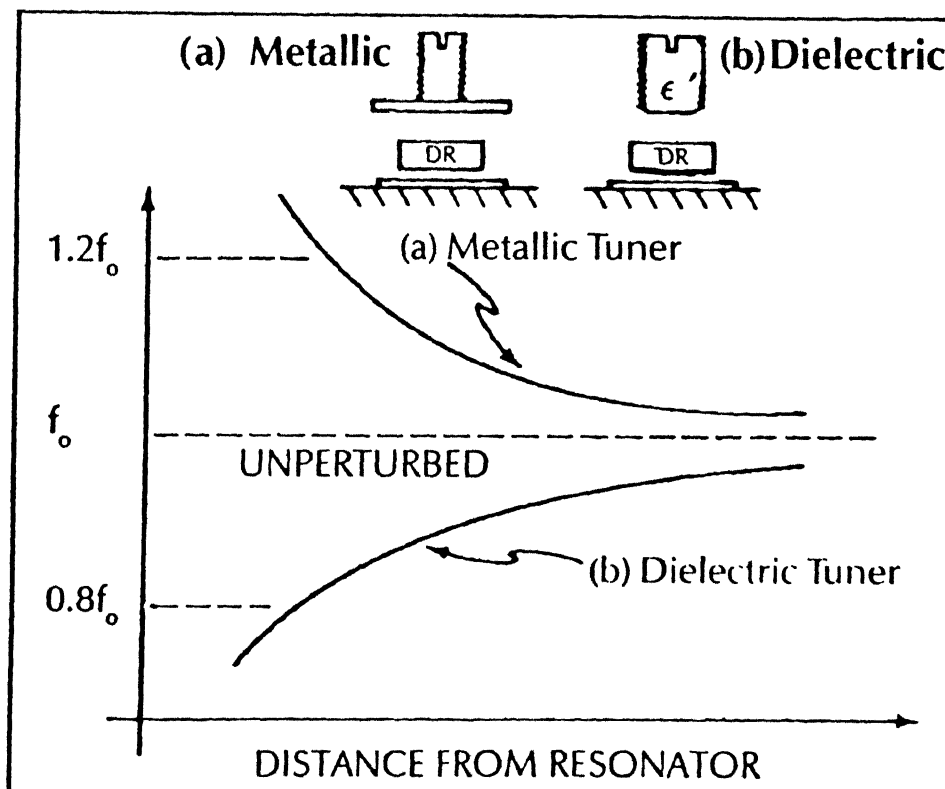


Fig. 2.7: Tuning by stub method [12]

Chapter 3

ENERGY DISTRIBUTION OF DIELECTRIC RESONATOR IN SUSPENDED SUBSTRATE ENVIRONMENT

The relative energy distributions in different regions of the circuit structure involving dielectric resonator, is very useful in deciding how to couple to the resonator. This chapter will deal with electrical and magnetic energy distribution for TE_{01δ} mode at resonance.

3.1 Electrical Energy Distribution

Total electrical energy stored in a structure given in Fig. 2.1 is the sum of individual electrical energy stored in each region. It may be calculated from field expressions derived in chapter 2.

$$W_e = \sum_{i=1}^8 W_{ei} \quad (3.1)$$

here W_{ei} is the electric energy stored in the i^{th} region of the structure occupying volume V and having dielectric constant ϵ_{ri} . W_{ei} is given by

$$W_{ei} = \frac{\epsilon_0 \epsilon_{ri}}{2} \int_V |\underline{E}_i|^2 dv \quad (3.2)$$

For TE_{01δ} mode only E_ϕ component of electric field exists so for different regions we get stored electrical energy as follows:

For region 1

$$W_{e1} = \frac{\epsilon_0 \epsilon_d}{2} \int_0^d \int_0^{2\pi} \int_{-h/2}^{h/2} |E_{\phi 1}|^2 r dr d\phi dz \quad (3.3)$$

region 2

$$W_{e2} = \frac{\epsilon_o}{2} \int_0^d \int_0^{2\pi} \int_{h/2}^{d1} |E\phi_2|^2 r \, dr \, d\phi \, dz \quad (3.4)$$

region 3

$$W_{e3} = \frac{\epsilon_o \epsilon_{s1}}{2} \int_0^d \int_0^{2\pi} \int_{-d3}^{-h/2} |E\phi_3|^2 r \, dr \, d\phi \, dz \quad (3.5)$$

region 4

$$W_{e4} = \frac{\epsilon_o \epsilon_{s2}}{2} \int_0^d \int_0^{2\pi} \int_{-d2}^{-d3} |E\phi_4|^2 r \, dr \, d\phi \, dz \quad (3.6)$$

region 5

$$W_{e5} = \frac{\epsilon_o}{2} \int_d^{ts} \int_0^{2\pi} \int_{h/2}^{d1} |E\phi_5|^2 r \, dr \, d\phi \, dz \quad (3.7)$$

region 6

$$W_{e6} = \frac{\epsilon_o}{2} \int_d^{ts} \int_0^{2\pi} \int_{-h/2}^{-h/2} |E\phi_6|^2 r \, dr \, d\phi \, dz \quad (3.8)$$

region 7

$$W_{e7} = \frac{\epsilon_o \epsilon_d}{2} \int_d^{ts} \int_0^{2\pi} \int_{-d3}^{-h/2} |E\phi_7|^2 r \, dr \, d\phi \, dz \quad (3.9)$$

region 8

$$W_{e8} = \frac{\epsilon_o \epsilon_d}{2} \int_d^{ts} \int_0^{2\pi} \int_{-d2}^{-d3} |E\phi_8|^2 r \, dr \, d\phi \, dz \quad (3.10)$$

here t_s is the saturation distance, i.e. after this distance in radial direction energy is zero.

After putting the values of fields from chapter 2, and solving integrals we get the expression for these electrical energies as follows:

$$W_{e1} = A0.A1234.\epsilon_d.A16 \quad (3.11)$$

$$W_{e2} = A0 . A1234 . B_2^2 . t_{same} (h_a, d_1, \alpha_a) \quad (3.12)$$

$$W_{e3} = A0 . A1234 . \epsilon_{s1} . B_3^2 . A37 \quad (3.13)$$

$$W_{e4} = A0 . A1234 . \epsilon_{s2} . B_5^2 . t_{same} (h_{s2}, d_2, \alpha_s) \quad (3.14)$$

$$W_{e5} = A0 . A5678 . B_6^2 . t_{same} (h_a, d_1, \alpha_a) \quad (3.15)$$

$$W_{e6} = A0 . A5678 . B_7^2 . A16 \quad (3.16)$$

$$W_{e7} = A0 . A5678 . \epsilon_{s1} . B_8^2 . A37 \quad (3.17)$$

$$W_{e8} = A0 . A5678 . \epsilon_{s2} . B_9^2 . t_{same} (h_{s2}, d_2, \alpha_s) \quad (3.18)$$

where,

$$A0 = \pi . \epsilon_o . (\omega_o \mu_o)^2 \quad (3.19)$$

$$A1234 = I_{ej} / k_r^2 \quad (3.20)$$

$$A5678 = I_{ek} / k_a^2 \quad (3.21)$$

Here constants B_i s are the same as in chapter 2, and are given in appendix A. Other constants are given in appendix B and C.

3.1.1 Electric Energy filling factor

Energy filling factor is an important quantity used in concern with the analysis of partially filled cavities. This is defined as the ratio of the electric energy for a given region to the total electric energy stored in the system. Based on the above analysis for electric energy, a program is developed to find the energy in all the regions. Results obtained are tabulated in terms of energy filling factor for each region for different dielectric constants of the resonator and substrate.

Table 3.1: Electric Energy Filling Factor for various regions of resonant structure in suspended substrate Environment

($d=0.9648\text{mm}$, $h=0.684\text{mm}$, $h_{s1}=0.79\text{mm}$, $h_{s2}=2.0\text{mm}$, $h_a=3.0\text{mm}$, $\epsilon_{s2}=1.0$)

ϵ_d	ϵ_{s1}	Energy filling factor(= W_{e1}/W_e)% for region no.							
		1	2	3	4	5	6	7	8
29.4	2.22	97.5	0.44	1.04	.005	.096	.733	0.23	.001
35.0	2.22	97.9	0.36	0.86	.004	0.08	0.61	0.19	.008
29.4	10.0	96.1	0.42	2.49	.004	0.08	.495	0.45	.000

It can be observed from Table 3.1. that for $\epsilon_d = 35.0$, most of the electrical energy (97.8%) is confined within the resonator. Energy leakage in region increases when dielectric constant of the DR decreases. Similarly using higher dielectric constant substrate, energy contents in the region 3 and 7 increase. But, in all cases more than 96% electrical energy is stored in the resonator.

3.2 Magnetic energy distribution

As we have seen from previous description that for high dielectric constant resonators, more than 96% electrical energy is confined within the resonator for $TE_{01\delta}$ mode, hence, electrical coupling of the DR with other circuit components is very week. We can also find magnetic energy of the structure in the same way as we have done for electrical energy. The net magnetic energy is the sum of magnetic energies of individual regions.

$$W_m = \sum_{i=1}^8 W_{m1} \quad (3.34)$$

Here W_{m1} is the magnetic energy stored in the i^{th} region of

the structure (Fig. 2.1), occupying volume V , and having relative permeability μ_{r1} . W_{m1} is given by

$$W_{m1} = \frac{\mu_0 \mu_{r1}}{2} \int_V |\underline{H}_1|^2 dv \quad (3.35)$$

For TE₀₁ δ mode only H_r and H_z components of magnetic field exists. So,

$$|\underline{H}_1|^2 = \underline{H}_1 \cdot \underline{H}_1^* = H_{r1}^2 + H_{z1}^2 \quad (3.36)$$

And for different regions we can write as follows:

For region 1

$$W_{m1} = \frac{\mu_0}{2} \int_0^d \int_0^{2\pi} \int_{-h/2}^{h/2} \{H_{r1}^2 + H_{z1}^2\} r dr d\phi dz$$

region 2

$$W_{m2} = \frac{\mu_0}{2} \int_0^d \int_0^{2\pi} \int_{h/2}^{d1} \{H_{r2}^2 + H_{z2}^2\} r dr d\phi dz$$

region 3

$$W_{m3} = \frac{\mu_0}{2} \int_0^d \int_0^{2\pi} \int_{-d3}^{-h/2} \{H_{r3}^2 + H_{z3}^2\} r dr d\phi dz$$

region 4

$$W_{m4} = \frac{\mu_0}{2} \int_0^d \int_0^{2\pi} \int_{-d2}^{-d3} \{H_{r4}^2 + H_{z4}^2\} r dr d\phi dz$$

region 5

$$W_{m5} = \frac{\mu_0}{2} \int_d^{ts} \int_0^{2\pi} \int_{h/2}^{d1} \{H_{r5}^2 + H_{z5}^2\} r dr d\phi dz$$

region 6

$$W_{m6} = \frac{\mu_0}{2} \int_d^{ts} \int_0^{2\pi} \int_{-h/2}^{h/2} \{H_{r6}^2 + H_{z6}^2\} r dr d\phi dz$$

region 7

$$W_{m7} = \frac{\mu_o}{2} \int_d^{t_s} \int_0^{2\pi} \int_{-d_3}^{-h/2} \{H_{r7}^2 + H_{z7}^2\} r dr d\phi dz$$

region 8

$$W_{m8} = \frac{\mu_o}{2} \int_d^{t_s} \int_0^{2\pi} \int_{-d_2}^{-d_3} \{H_{r8}^2 + H_{z8}^2\} r dr d\phi dz$$

Here, t_s is the saturation distance, i.e. after this distance in radial direction energy is zero.

After putting the values of fields from chapter 2, and solving integrals we get the expression for these electrical energies as follows:

$$W_{m1} = A'0 \{A'1234.A16 + \beta_1^2.A1234.A'16\}$$

$$W_{m2} = A'0.B_2^2 \{A'1234.t_{same}(h_a, d_1, \alpha_a) + \alpha_a^2.A1234.t'_{same}(h_a, d_1, \alpha_a)\}$$

$$W_{m3} = A'0.B_3^2 \{A'1234.A37 + \beta_2^2.A1234.A'37\}$$

$$W_{m4} = A'0.B_5^2 \{A'1234.t_{same}(h_{s2}, d_2, \alpha_s) + \alpha_s^2.A1234.t'_{same}(h_{s2}, d_2, \alpha_s)\}$$

$$W_{m5} = A'0.B_6^2 \{A'5678.t_{same}(h_a, d_1, \alpha_a) + \alpha_a^2.A5678.t'_{same}(h_a, d_1, \alpha_a)\}$$

$$W_{m6} = A'0.B_7^2 \{A'5678.A16 + \beta_1^2.A5678.A'16\}$$

$$W_{m7} = A'0.B_8^2 \{A'5678.A37 + \beta_2^2.A5678.A'37\}$$

$$W_{m8} = A'0.B_9^2 \{A'5678.t_{same}(h_{s2}, d_2, \alpha_s) + \alpha_s^2.A5678.t'_{same}(h_{s2}, d_2, \alpha_s)\}$$

(3.37)

where

$$A'0 = \mu_o \Pi$$

$$A'1234 = I_{j0}/k_r^2$$

$$A'5678 = I_{k0}/k_a^2$$

(3.38)

and other constants are given in appendix B and C.

3.2.1 Magnetic Energy Filling Factor

This factor for a region represents the part of total magnetic energy in that region. For TE_{01δ} mode it is of great importance, because, the coupling is mainly magnetic energy coupling in this mode. Table 3.2 is showing the magnetic energy distribution in all the regions of the structure.

Table 3.2: Magnetic Energy Filling Factor for various regions of resonant structure in suspended substrate Environment

($d=0.9648\text{mm}$, $h=0.684\text{mm}$, $h_{s1}=0.79\text{mm}$, $h_{s2}=2.0\text{mm}$, $h_a=3.0\text{mm}$, $\epsilon_{s2}=1.0$)

ϵ_d	ϵ_{s1}	Energy filling factor(= W_{m1}/W_m)% for region no.							
		1	2	3	4	5	6	7	8
29.4	2.22	58.1	13.78	14.2	.15	2.5	8.67	2.55	.03
35.0	2.22	58.3	13.76	14.1	.14	2.47	8.7	2.5	.03
29.4	10.0	63.8	15.81	7.04	.17	2.55	9.54	1.1	.03

We can observe from above Table 3.2 that in any case near about 38% of the magnetic energy is distributed out of the resonator. Therefore, strong coupling between resonators and other components can be achieved by placing the component in the region of higher magnetic energy. For this purpose region no. 2 and 6 can be used for strong coupling and for weak coupling requirements region no. 4 or 8 can be used.

The information presented in this chapter is very useful from design point of view. It will be used in proceeding chapters.

Chapter 4

COUPLING BETWEEN TWO SYMMETRICAL DIELECTRIC RESONATORS IN SUSPENDED SUBSTRATE

The design of microwave circuits, involving dielectric resonators like band pass or band reject filters, basically involves two design issues: the first one is the *input/output* coupling and the second is the *interstate* coupling. Interstate coupling, which provides transfer of energy from one resonator to another resonator either directly or through another transmission line, is presented in this chapter.

Analysis presented in the next chapter may be extended for calculating the coupling between two resonators coupled via a section of suspended stripline, micro stripline or inverted microstrip line. In this chapter we derive the analytical formulation for the coupling coefficient between two directly coupled DRs, for three very important configurations viz. edge coupled, off-layered and broad-side coupled resonators.

4.1 Direct coupled Cylindrical Resonators

Two cylindrical resonators may be coupled directly in $TE_{01\delta}$ mode by placing them over a suspended substrate adjacent to each other as shown in the Fig. 4.1. The degree of coupling is mainly determined by the lateral distance S between them. As both resonators are assumed to be operate in the $TE_{01\delta}$ mode, interaction between them occurs through magnetic field lines, because, most of the electric field is confined within the resonators itself. Due to this magnetic interaction, resonators may be assimilated as *magnetic dipole*, formed by small current loops.

Fig.4.2 shows the side view of two cylindrical resonators placed at a distance of S . From this figure we observe that first resonator is placed in the sixth region (refer to Fig. 2.1) of the second resonator and vice versa. As we have Assumed both resonators to be identical (in dimension and material properties), each of them may be represented by a conducting loop having self inductance L_r resonating with capacitance C_r at the resonant frequency f_0 . Magnetic field interaction between the resonators is characterized by mutual inductance L_m . In circuit theory, the coupling coefficient k is defined as

$$k = \frac{L_m}{L_r} \quad (4.1)$$

Here, we are representing the resonators by equivalent current loops and the voltage induced in loop 2 is due to current I_{r1} flowing in loop 1. In terms of circuit quantities this induced voltage may be expressed as

$$V_2 = - L_m \frac{dI_{r1}}{dt} = -j\omega_0 L_m I_{r1} \quad (4.2)$$

Value of the magnetic energy stored of the resonator 1 is given by

$$W_{m1} = \frac{1}{2} L_r I_{r1}^2 \quad (4.3)$$

From eqs. (4.1) and (4.2) we get

$$\frac{L_m}{L_r} = - \frac{V_2 I_{r1}}{2j\omega_0 W_{m1}} \quad (4.4)$$

Induced voltage in loop 2, according to Faraday's law, may be written in terms of field quantities as

$$V_2 = - \oint_c \underline{E}^1 \cdot d\underline{l} = j\omega_0 \mu_0 \oint \underline{H}^1 \cdot d\underline{s} \quad (4.5)$$

here, \underline{E}^1 and \underline{H}^1 are fields in place of the second resonator due to first resonator, and surface ' s ' is the area in

second DR and substrate through which magnetic lines crosses perpendicularly. 'c' is the contour enclosing the surface 's'. Here it is assumed that voltage induced in the one resonator is only due to the current flowing in the other resonator.

From reaction concept it comes that

$$\oint_{c'} \underline{E}^1 \cdot d\underline{l} = \int_v \underline{E}^1 \cdot \underline{J} dv \quad (4.6)$$

where \underline{J} is the current density in the volume of second resonator.

From eqs (4.1) to (4.6), we get the expression for coupling coefficient as follows:

$$k = \frac{\iiint_v \underline{E}^1 \cdot \underline{J} dv}{2j \omega_0 W_{m1}} \quad (4.7)$$

If current loops are replaced by original DRs in the above analysis then, current density \underline{J} becomes equal to polarization current \underline{J}_p present in volume v. In the present context \underline{J}_p is expressed as

$$\underline{J}_p = j\omega_0 \epsilon_0 \{ (\epsilon_d - 1) \underline{E}^2 + (\epsilon_{s1} - 1) \underline{E}^2 + (\epsilon_{s2} - 1) \underline{E}^2 \} \quad (4.8)$$

where \underline{E}^2 is electric field of the second resonator in volume v. For TE₀₁δ mode only E_φ component of electric field exist, so, eqs (4.8) reduces to

$$\underline{J}_p = j\omega_0 \epsilon_0 \{ (\epsilon_d - 1) E_{\phi}^2 + (\epsilon_{s1} - 1) E_{\phi}^2 + (\epsilon_{s2} - 1) E_{\phi}^2 \} \hat{1}_{\phi} \quad (4.9)$$

For calculation of coupling coefficient using (4.7) at given resonant frequency f_0 , we need to find out two things. They are the magnetic energy stored (W_{m1}) due to excited resonator and the volume integral which changes according to placement of second resonator. W_{m1} which remain constant for fixed structural parameters, can be obtained from previous

chapter. Here we will present the volume integral for three stated configurations.

4.1.1 Edge-coupled Resonators

For edge coupled resonators (Fig. 4.2), the volume integral can be written in the form of

$$\iiint \underline{E}^1 \cdot \underline{J} \, dv = \frac{j\omega_0 \epsilon_0 (\omega_0 \mu_0)^2}{k_a \cdot k_r} [(\epsilon_d - 1) B_7 A_{16} + (\epsilon_{s1} - 1) B_3 B_8 A_{37} + (\epsilon_{s2} - 1) B_5 B_9 t_{same}(h_{s2}, d_2, \alpha_s)] I_{jk} \quad (4.10)$$

The value of constants are given in Appendix A, B and C. By substituting the values of volume integral from eqs.(4.10) to eqs. (4.7), we get formulation for coupling coefficient between two DRs placed on the upside of the suspended substrate (Fig. 4.1).

4.1.2 Coupling between two DRs placed on Opposite sides of Suspended substrate

We have extended this theory for getting coupling coefficient between two DRs, placed either side of the suspended substrate (Fig. 4.4) by replacing the two DRs with two equivalent current loops. The current flowing in one loop will generate the magnetic flux, which will be linked to the second loop through the substrate. The change in magnetic flux will give rise to induced voltage in second loop. We have assumed both DRs to be identical in properties and dimensions, and the formulation is derived for symmetrical location of DRs on the suspended substrate (i.e., $h_{s2} = h_a + h_{s1}$, and $\epsilon_{s2} = 1.0$), for two configurations of Fig. 4.4. The volume integral for above mentioned configurations can be given as

$$\iiint \underline{E}^1 \cdot \underline{J} \, dv = \frac{j\omega_0 \epsilon_0 (\omega_0 \mu_0)^2}{k_a \cdot k_r} [(\epsilon_d - 1.0) \cdot e^{-\alpha \cdot d_2} \cdot B_9 \cdot A_{18} + (\epsilon_{rs} - 1.0) \cdot B_3 \cdot B_8 \cdot A_{37} d] \cdot I_{jk} \quad (4.11)$$

for off-layered case.

and,

$$\iiint \underline{E}^1 \cdot \underline{J} \, dv = 2\pi \frac{j\omega_0 \epsilon_0 (\omega_0 \mu_0)^2}{k_r \cdot k_r} [(\epsilon_d - 1.0) \cdot e^{-\alpha_s \cdot d^2} \cdot B_5 \cdot A18 + (\epsilon_{s1} - 1.0) \cdot B_3 \cdot A37d^2] \cdot I_e \quad (4.12)$$

for broad side case.

The value of constants appearing in these expressions are given in appendix A, B and C.

By substituting the value of volume integrals from eqs (4.12) and (4.13) into the eqs (4.7), we can obtain the coupling coefficient for two cases given in Fig.4.4.

4.2 Numerical Results

We have validated the present method, by calculating the coupling coefficient between DRs for given structural parameters [30], in microstrip line as a special case of the suspended stripline. In our present calculation we calculated frequency and other eigen values from EDC method. These theoretical results shows a good agreement with the experimental data presented in [30] and can be seen in Fig. 4.3.

Fig. 4.5 shows the variation of the coupling coefficient between two edge coupled dielectric resonators placed in suspended substrate, as a function of edge to edge separation 'S' between them, for Ka band. It is clear from this graph that the coupling coefficient k is very strong function of separation S between the resonators. Hence, spacing between resonators should be determined very accurately in practical applications.

Fig. 4.6 is showing the coupling coefficient variation with change in separation (S) between two Drs, for off layered coupling (Fig. 4.4a). We see that the coupling coefficient k is a strong function of the separation between the DRs, and it decreases very rapidly as we increase the separation between two DRs. It also shows that for same dimensions of the structure, the coupling increases as we

increase the dielectric constant(ϵ_{rs}) of the substrate. We also find that the coupling is weak even for zero separation($S=0$), compared to that in edge coupled case (Fig.4.2).

Fig. 4.7 is showing the change in the coupling coefficient with change in the width of the substrate(h_{s1}), for the Broadside coupling (Fig.4.4b). It shows that the coupling is decreasing with increase in the thickness of the substrate. It also shows that very tight coupling can be achieved in the Broadside case.

We conclude from the above figure that off layered coupling between DRs (Fig. 4.4a), can be used for the purpose of weak coupling and the Broadside structure (Fig. 4.4b) can be used for very tight coupling. The most important advantage of these structures is that we can miniaturize the microwave circuits, involving the DRs for tight as well as weak coupling purposes.

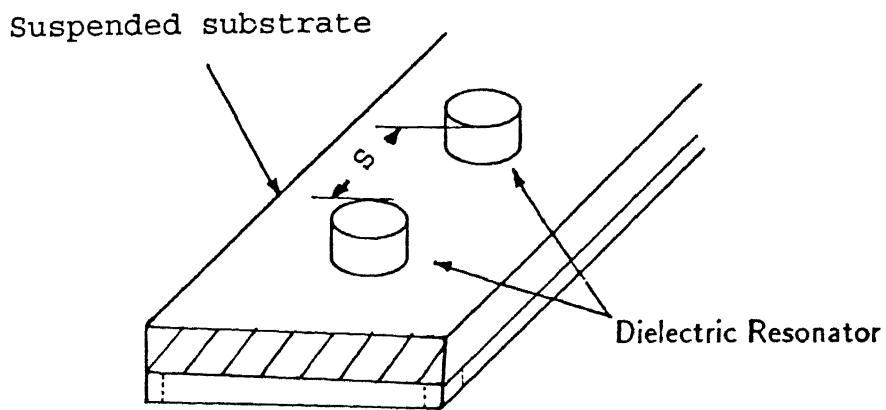


Fig. 4.1: Two directly coupled resonators on the same side of suspended substrate

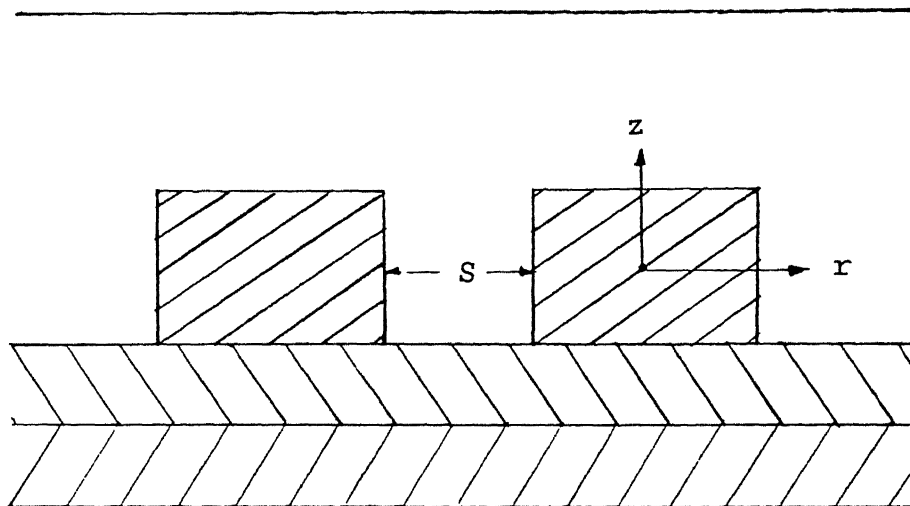


Fig. 4.2: Side view of two edge coupled dielectric resonators

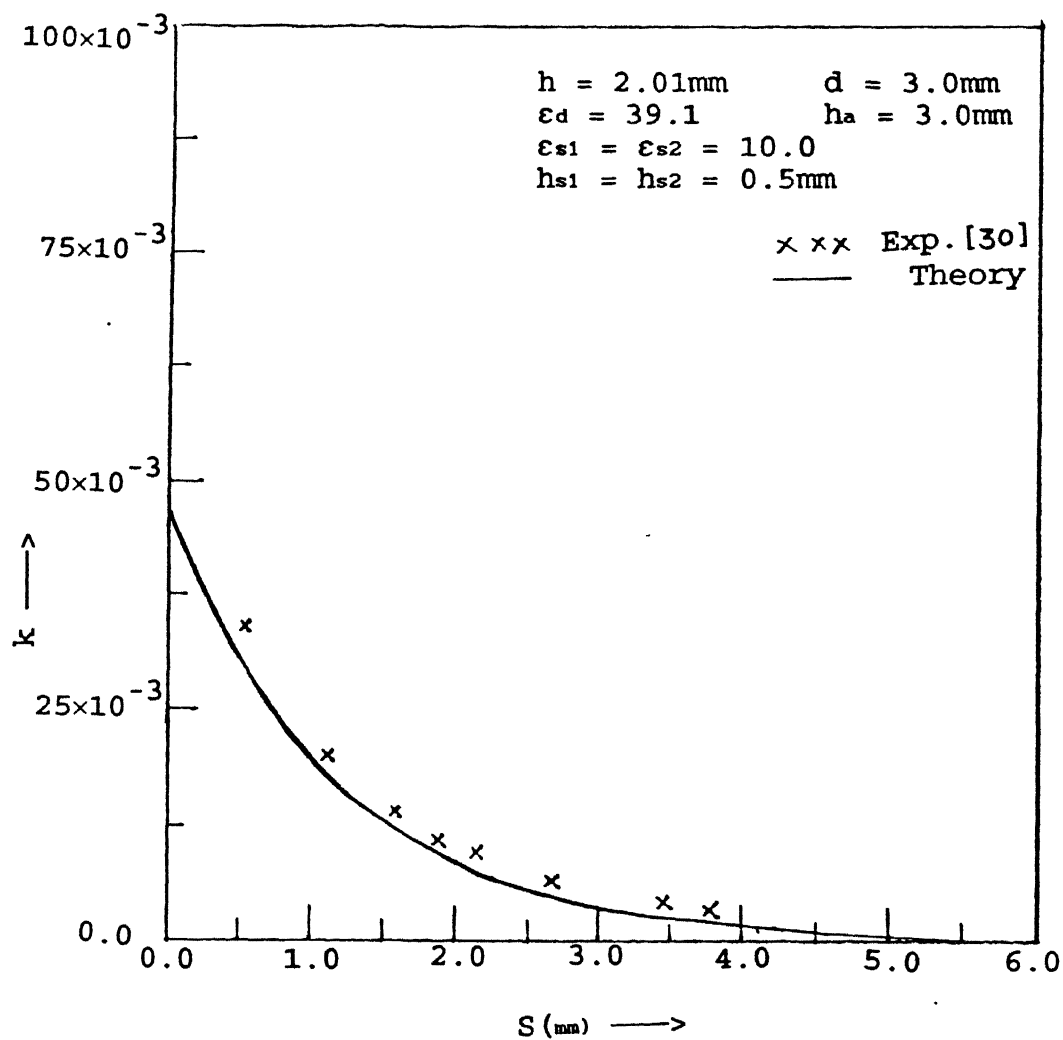


Fig. 4.3: Comparison of theoretical results with experimental data for microstrip configuration

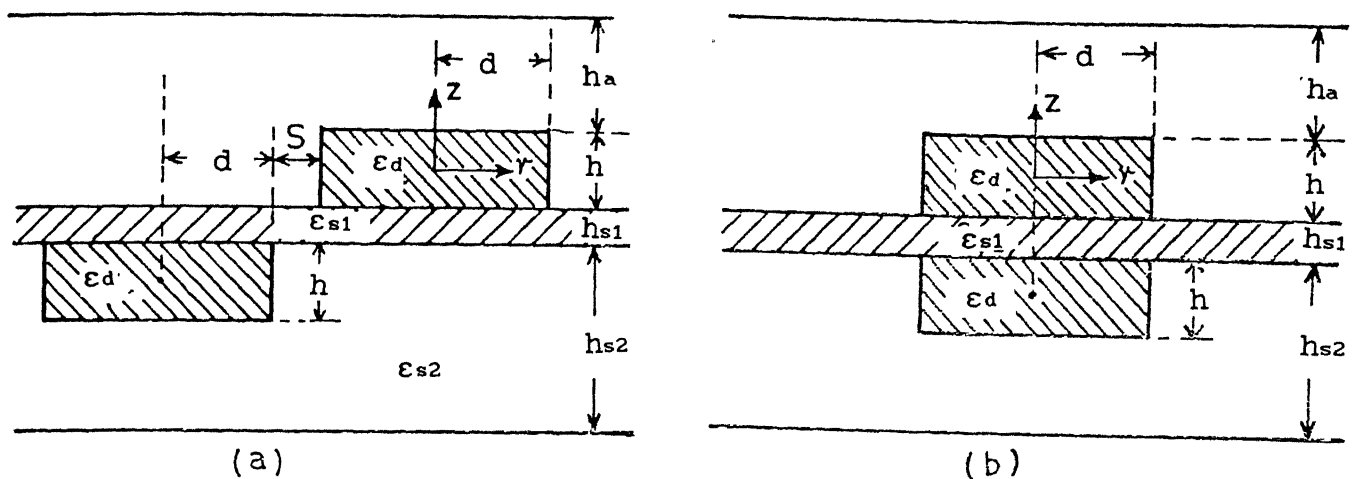


Fig. 4.4: Coupling between two DRs placed on opposite sides of suspended substrate. (a) Off-layered coupling, (b) Broad side coupling.

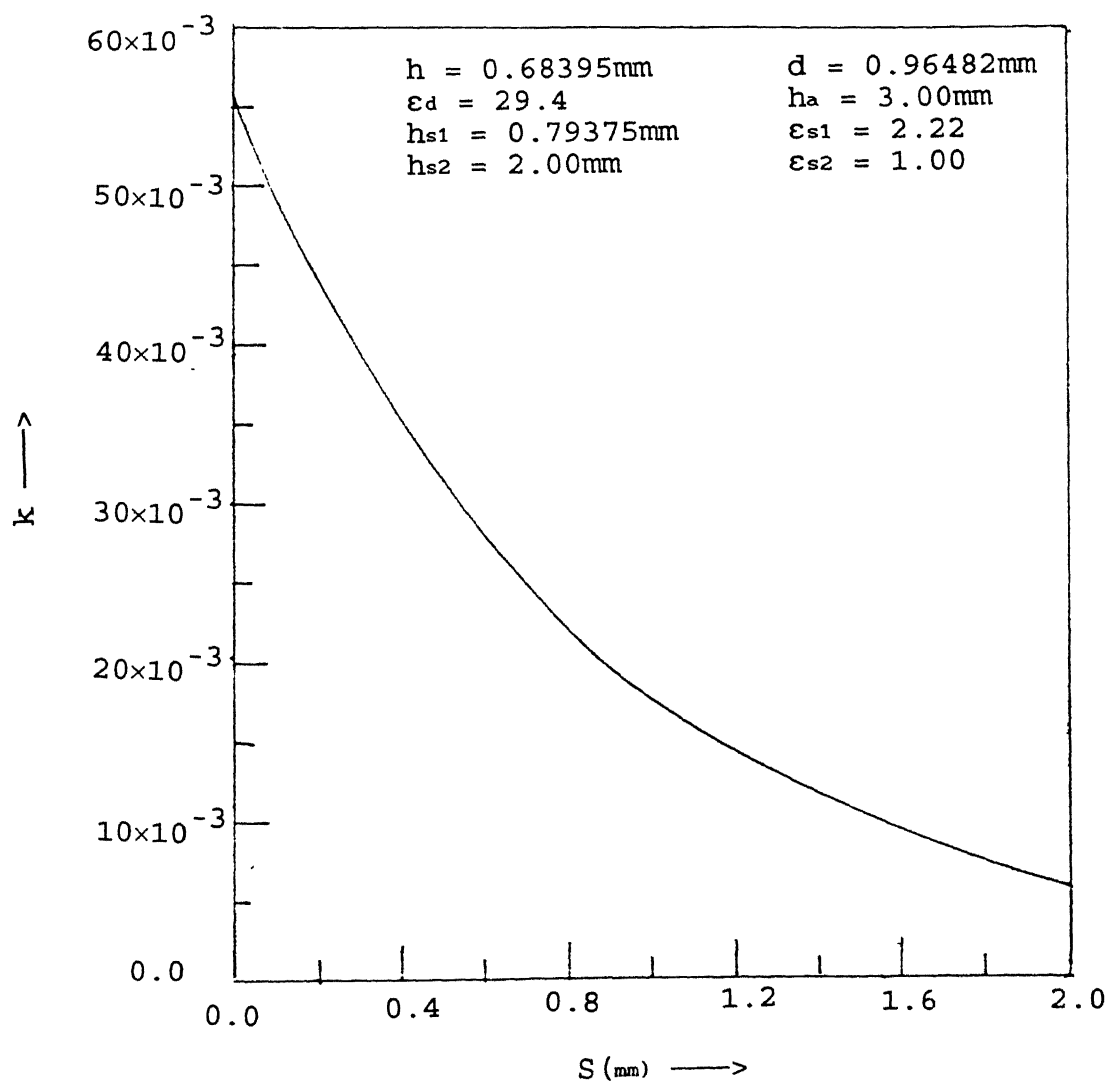


Fig. 4.5: Coupling coefficient between two edge-coupled DRs as function of separation S between them

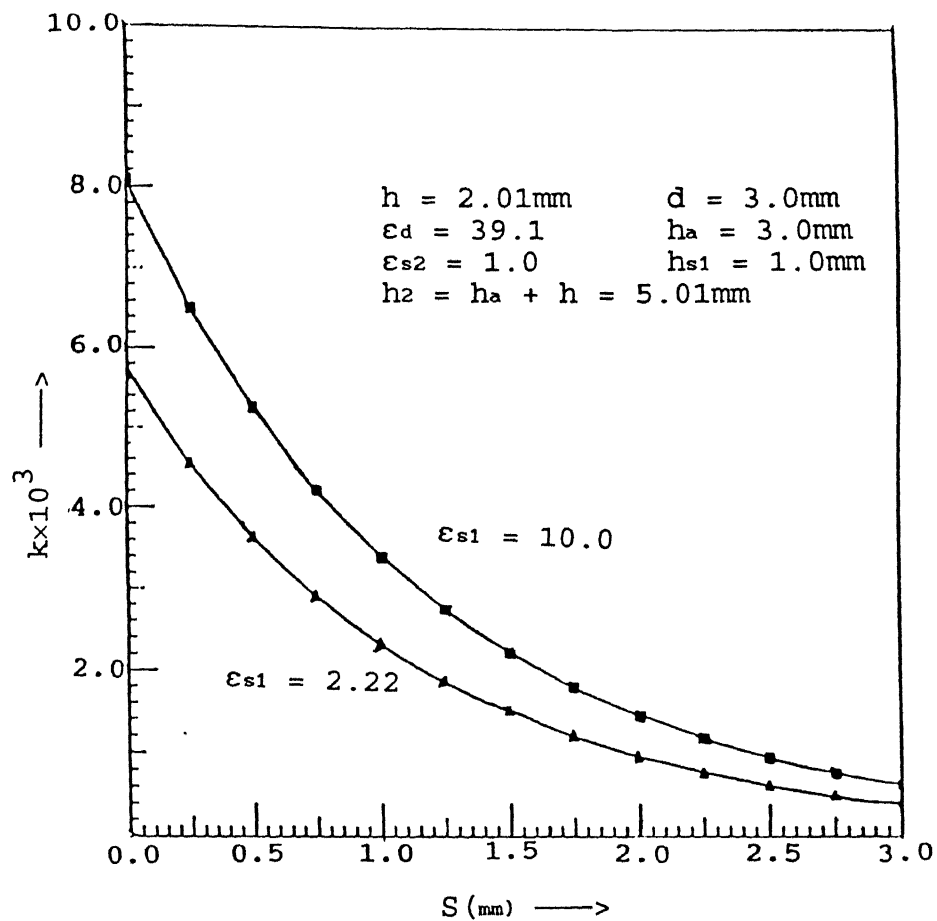


Fig. 4.6 Coupling coefficient for off-layered DRs as Function of separation between DRs.

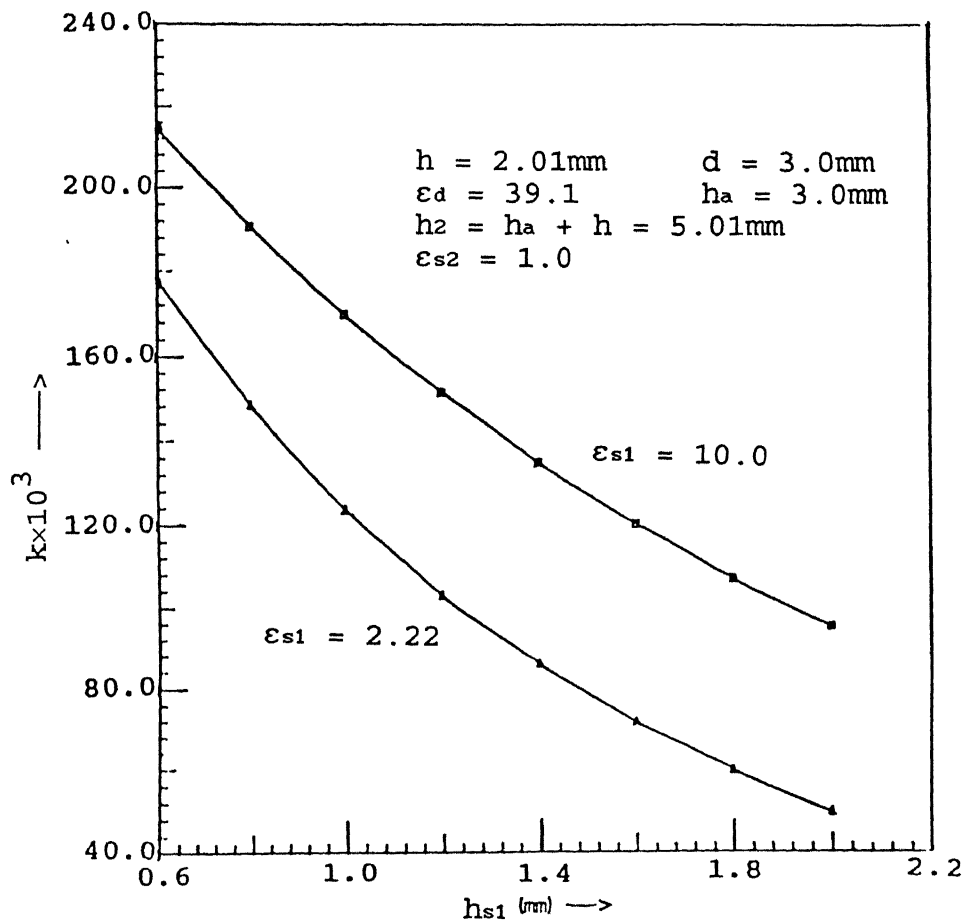


Fig. 4.7 Coupling coefficient for Broadside case as a function of the thickness of the substrate.

Chapter 5

COUPLING BETWEEN DIELECTRIC RESONATOR AND STRIP-CONDUCTOR WITH FINITE THICKNESS ON SUSPENDED SUBSTRATE

As we have mentioned in earlier chapter that there are two types of viz. *interstate* coupling and *input/output* coupling . The input/output coupling is the coupling between the resonator and a transmission line which either excites the resonator or extracts the electromagnetic energy from the resonator. Many types of transmission lines like co-axial probe, current loop, waveguides, stripline, microstrip line, etc. can be used for this purpose. Coupling between a cylindrical dielectric resonator (DR) and a strip conductor with finite thickness (t), for $TE_{01\delta}$ mode in suspended substrate environment, is the subject matter in this chapter.

5.1 Methods of coupling for $TE_{01\delta}$ and $TM_{01\delta}$ modes

The $TE_{01\delta}$ and $TM_{01\delta}$ are most commonly used modes, which can be easily excited in dielectric resonator using microstrip line, fin line, magnetic loop, metallic and dielectric waveguides, microstrip line, suspended stripline etc. [8]. Field configurations in these modes are such that resonator operating in any of these modes can be modeled in terms of low frequency lumped elements.

Fig. 5.1(a) shows the magnetic field distribution for $TE_{01\delta}$ mode and various methods for coupling of this mode. Electric field lines for this mode are simple circles concentric with the axis of the cylindrical resonator. When the dielectric constant is around 40, more than 96% of the stored electric energy as well as a great part of magnetic energy (typically 60%) is confined within the resonator. The remaining energy, distributed in the surrounding of the DR,

is decaying rapidly with distance away from the resonator surface. As seen from this figure, for a distant observer this mode appears as a small magnetic dipole formed by a small coil, and for this reason some authors call it a *magnetic dipole mode* instead of using the term $TE_{01\delta}$ introduced by Cohn [14].

Coupling to this mode is often accomplished through the magnetic field via a small horizontal loop placed in the plane parallel to the flat surface of the DR or by placing the end face of the DR near a strip conductor of planar transmission line like microstrip line or suspended stripline (Fig. 5.19(a)), so that the magnetic lines of the DR link with those of the loop or the strip-conductor. Coupling of a resonator to a waveguide operating in the TE_{01} mode can be accomplished by placing the resonator axially within the waveguide. Coupling to this mode via electric field can also be obtained using a small horizontal dipole or a bent monopole as illustrated in the figure.

$TM_{01\delta}$ mode is dual of $TE_{01\delta}$ mode. Role of electric and magnetic field gets interchanged in this mode (Fig. 5.1(b)). Magnetic field is well confined within the resonator and electric field is strong near the axis of the resonator. Coupling to this mode can be accomplished in different ways as shown in Fig. 5.1(b). A probe, well aligned with the axis of the resonator effectively couples the electric field. Coupling to strip conductor of planar transmission line can be accomplished by placing the resonator on its side with its axis of rotation parallel to the strip conductor so that the magnetic field lines loop around the strip conductor. The resonator may be coupled to the TE_{01} waveguide mode by placing it on its end in the waveguide as implied by the orientation of the waveguide in the figure.

5.2 Coupling between DR and planar Transmission lines

Microstrip line is the most popular transmission line used with cylindrical resonators, in microwave integrated

circuits (MICs), operating at lower frequency band. But, at higher frequencies, specially in millimeter (mm) wave range, the microstrip line fails to satisfy the requirements of losses, fabrication tolerances and handling fragility etc., and also, it becomes very dispersive in nature. The supplements to these requirements are suspended stripline and microstrip line, for mm wave applications. Hence it is necessary to characterize quantitatively this coupling between a DR and two important transmission line structures like suspended stripline and inverted microstrip line. Our next sections are devoted to this transmission line to dielectric resonator transition.

One way to incorporate the dielectric resonator in a microwave circuit is by placing it on the suspended substrate having the strip conductor of a planar transmission line, as shown in Fig. 5.2.

When a DR is placed in the vicinity of a transmission line, as shown in Fig. 5.2, and excited in the $TE_{01\delta}$ mode, the transmission characteristics of the line are modified by the magnetic effect. The electric effect caused by the high dielectric constant DR can be assumed to be very small, since most of the transmission line is not only concentrated under the strip conductor but also almost orthogonal to the electric field of the DR [31]. The magnetic effect is an interaction between the magnetic field of the resonator and the magnetic field owing to the current in the strip conductor. This interaction can be regarded as mutual inductance L_m , and an emf is considered to be caused in the strip conductor.

For this coupling the lateral distance between the strip conductor and resonator primarily determines the degree of coupling. Termination of the strip conductor and proper shielding also plays an important role in determining amount of coupling.

Analysis

Since the analysis of the configurations shown in the Fig.

5.2 is a formidable problem, an approximate method given by Guillon [32] and Komatsu [31] is used for analysis.

The analysis is made on the basis of the following assumptions [31].

1. The width of the strip conductor is much smaller than the diameter of the resonator.
2. The transmission line carries only the TEM mode.
3. The DR can be represented by a conducting loop having in series an inductance L_r , a capacitance C_r and a resistance R_r . The resonance occurs at the frequency $f_0 = 1/\sqrt{(L_r C_r)}$.
4. Only the $TE_{01\delta}$ mode is strongly excited and field distortion caused by other modes is very small.
5. The DR couples with transmission line through distributed mutual inductance L_m .

With these assumptions, the structures of Fig. 5.2 can be represented by a resonance circuit magnetically coupled with a transmission line as shown in Fig. 5.3, Where L_1 , C_1 and R_1 are, respectively, equivalent circuit parameter for the transmission line terminated in Z_1 and Z_0 at load and feeding ends of it, respectively. Let I_r and I_1 be the current flowing in the resonator and transmission line respectively. Applying KVL to this low frequency model we get

$$V = I_1 R_1 + j\omega L_1 I_1 + j\omega L_m I_r + \frac{I_1}{j\omega C_1} \quad (5.1)$$

$$0 = I_r R_r + j\omega L_r I_r + j\omega L_m I_1 + \frac{I_r}{j\omega C_r} \quad (5.2)$$

eliminating I_r we get

$$V = R_1 I_1 + j\omega L_1 I_1 + \frac{\omega^2 L_m^2 I_1}{R_r + j\omega L_r + 1/j\omega C_r} + \frac{I_1}{j\omega C_1} \quad (5.3)$$

The transfer impedance Z_t , in the coupling plane is obtained as

$$Z_t = \frac{V}{I_1} = R_1 + j\omega L_1 + \frac{\omega^2 L_m^2}{R_r + j\omega L_r + 1/j\omega C_r} + \frac{1}{j\omega C_1} \quad (5.4)$$

For perfect strip conductor R_1 is very small and near resonance $j\omega L_1 + 1/(j\omega C_1)$ may be neglected in comparison to terms containing ω^2 . Hence, the expression for Z_t reduces to

$$Z_t = \frac{\omega^2 L_m^2}{R_r + j \frac{(L_r)}{\omega} \{ \omega^2 - 1/(L_r C_r) \}} \quad (5.5)$$

Near resonance at $\omega = \omega_0 + \delta\omega$ transfer impedance may be written as

$$Z_t = \frac{(\omega_0 + \delta\omega)^2 L_m^2}{R_r + j \frac{(L_r)}{\omega_0 + \delta\omega} \{ (\omega_0 + \delta\omega)^2 - 1/(L_r C_r) \}} \quad (5.6)$$

Further simplification of Z_t is obtained by neglecting $(\delta\omega)^2$ and $(\delta\omega)/\omega_0$ terms

$$\begin{aligned} Z_t &= \frac{(\omega_0 + \delta\omega)^2 L_m^2}{R_r + j \frac{(L_r)}{\omega_0 + \delta\omega} \{ \omega_0^2 + (\delta\omega)^2 + 2\omega_0\delta\omega - 1/(L_r C_r) \}} \\ &= \frac{\omega_0 L_m^2}{\frac{R_r}{\omega_0} + j \frac{2\delta\omega L_r}{\omega_0}} \end{aligned}$$

Putting $R_r = \omega_0 L_r / Q_0$ in above equation we get

$$\begin{aligned} &= \frac{\omega_0 L_m^2}{\frac{L_r}{Q_0} + j \frac{2\delta\omega Q_0}{\omega_0}} \\ Z_t &= \omega_0 \frac{L_m^2}{L_r} Q_0 \frac{1}{1 + jX} \quad (5.7) \end{aligned}$$

Where

$$X = \frac{2\delta\omega Q_0}{\omega_0}$$

Equation (5.7) indicates that the circuit shown in Fig. 5.3 can be represented by a simple parallel tuned circuit as shown in Fig. 5.4, where L , C and R are obtained as

$$R = \omega_0 Q_0 \frac{L_m^2}{L_r}$$

$$L = \frac{L_m^2}{L_r}$$

$$C = \frac{L_r}{L_m^2 \omega_0}$$

(5.8)

At resonance $\omega = \omega_0$, so

$$Z_t(\omega_0) = R = \omega_0 Q_0 \frac{L_m^2}{L_r} \quad (5.9)$$

here Q_0 is the unloaded quality factor of DR.

For this parallel tuned circuit an important figure of merit is external quality factor Q_e , which is the Q factor of the circuit when loading of circuit is only due to external R_{ext} . Quantitatively it is given by

$$Q_e = Q_0 \cdot \frac{R_{ext}}{R} \quad (5.10)$$

For our circuit, R_{ext} symbolizes the internal impedance (Z_0) of the source feeding to the line, and the load impedance (Z_1) of the line. So, $R_{ext} = (Z_1 + Z_0)$.

$$\begin{aligned} Q_e &= \frac{(Z_1 + Z_0)}{R} Q_0 \\ &= \frac{(Z_1 + Z_0)}{\omega_0} (L_r / L_m^2) \end{aligned} \quad (5.11)$$

For known values of Z_1 , Z_0 and ω_0 , the external quality factor Q_e can be evaluated if we calculate (L_r / L_m^2) . The crux of the problem lies in finding the quantity (L_r / L_m^2) in terms of distance between DR and strip conductor.

The DR acting in $TE_{01\delta}$ mode can be assimilated to a magnetic dipole. Let I_r be the current flowing in the loop,

then, the voltage induced in the microstrip line due this current is given by

$$e = -j\omega_0 L_m I_r \quad (5.12)$$

This induced voltage is also given by (Faraday's Law)

$$e = -j\omega_0 \mu_0 \int_s \underline{H} \cdot d\underline{s} \quad (5.13)$$

where \underline{H} is the magnetic field of the resonator and s , i.e. the surface of integration, is the surface perpendicular to the conductors passing into the substrate through which magnetic lines of \underline{H} field crosses the strip conductor.

from eqs. (5.12) and (5.13) we get

$$L_m = -\frac{\mu_0}{I_r} \int_s \underline{H} \cdot d\underline{s} \quad (5.14)$$

The magnetic energy stored due to DR is given by

$$W_m = (L_r I_r^2) / 2 \quad (5.15)$$

From eqs. (5.14) and (5.15) we can obtain

$$\frac{L_r}{L_m^2} = \frac{2 W_m}{\mu_0^2 \left\{ \int_s \underline{H} \cdot d\underline{s} \right\}^2} \quad (5.16)$$

Substituting the value of the expression from eqs. (5.16) into (5.11) we get

$$Q_e = -\frac{2 (Z_1 + Z_0) W_m}{\omega_0 \mu_0^2 \left\{ \int_s \underline{H} \cdot d\underline{s} \right\}^2} \quad (5.17)$$

Now we see that for two configurations of Fig 5.2, only the surface integral will change with separation between the DR and the strip conductor. And also it will have different expressions for two configurations. Evaluation of $\int \underline{H} \cdot d\underline{s}$ for both the configurations is given in appendix E, and the magnetic energy W_m was derived in chapter 3.

5.3 Numerical Results

5.3.1 Comparison with Experimental Data

For the validation of present approximate analytical method presented above, computed Q_e was compared with the experimental data [32] and shown in Fig. 5.5. Here, a 50- Ω microstrip line as a special case of suspended stripline, terminated its characteristic impedance at both ends is used for calculating Q_e . Good agreement between calculated and experimental results justifies the use of the approximate analytical method for design purpose.

5.3.2 Coupling between Suspended stripline and DR

Fig 5.6(a) and Fig5.7(a) are showing the variation of Q_e as a function of separation between the suspended stripline and DR, operating in S and K_a bands of microwave frequencies, respectively. There are three curves in each of the figures, for three different thicknesses of the strip conductor to show the effect of thickness on Q_e , including the zero thickness case.

5.3.3 Coupling between Inverted Microstripline and DR

Fig 5.6(b) and Fig 5.7(b) are showing the variation of Q_e as a function of separation between the inverted microstripline and DR, operating in S and K_a bands of microwave frequencies, respectively. There are three curves in each of the figures, for three different thicknesses of the strip conductor including the zero thickness case.

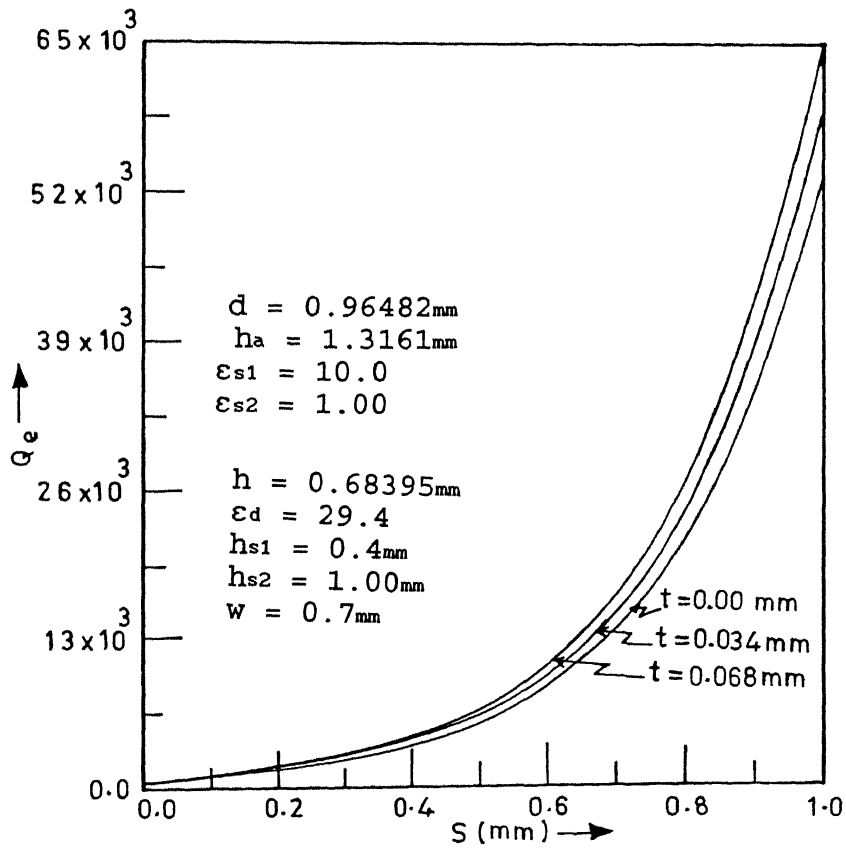
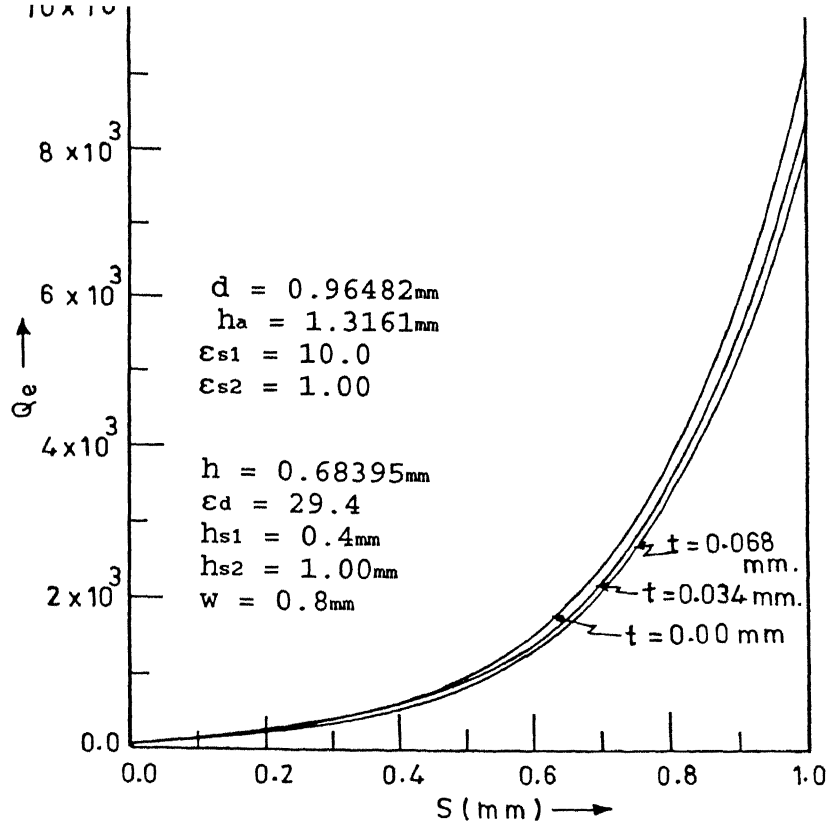
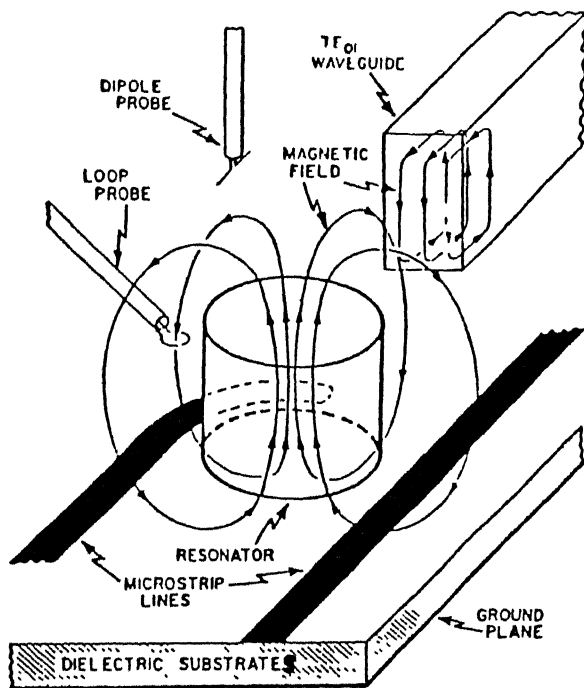
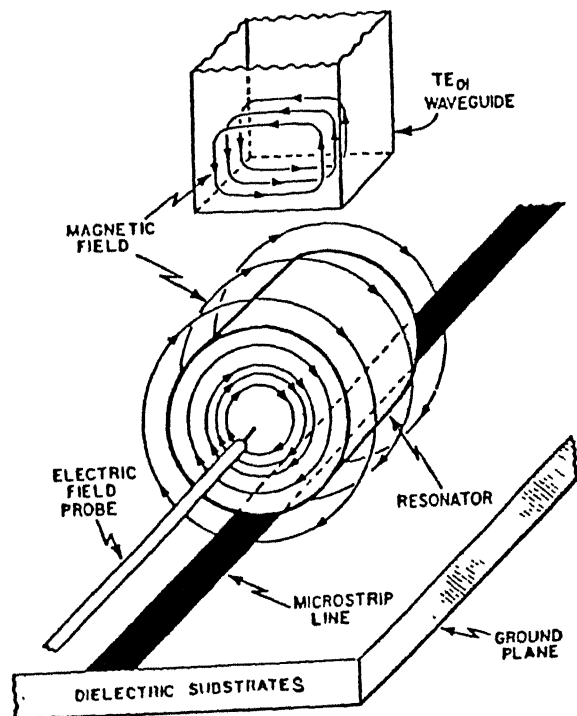


Fig. 5.7: Q_e 's variation as function of s for Ka-band (a) suspended stripline case. (b) inverted microstripline case



(a) $TE_{01\delta}$ mode



(b) $TM_{01\delta}$ mode

Fig. 5.1: Different methods of coupling to $TE_{01\delta}$ and $TM_{01\delta}$ mode [7]

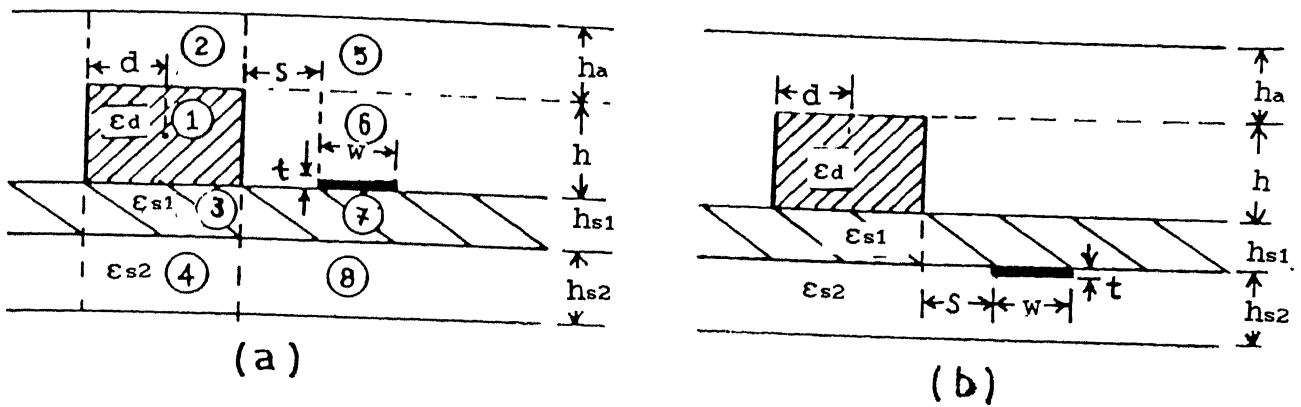


Fig. 5.2: Dielectric resonator coupled to transmission lines
 (a) Suspended stripline. (b) Inverted microstrip line

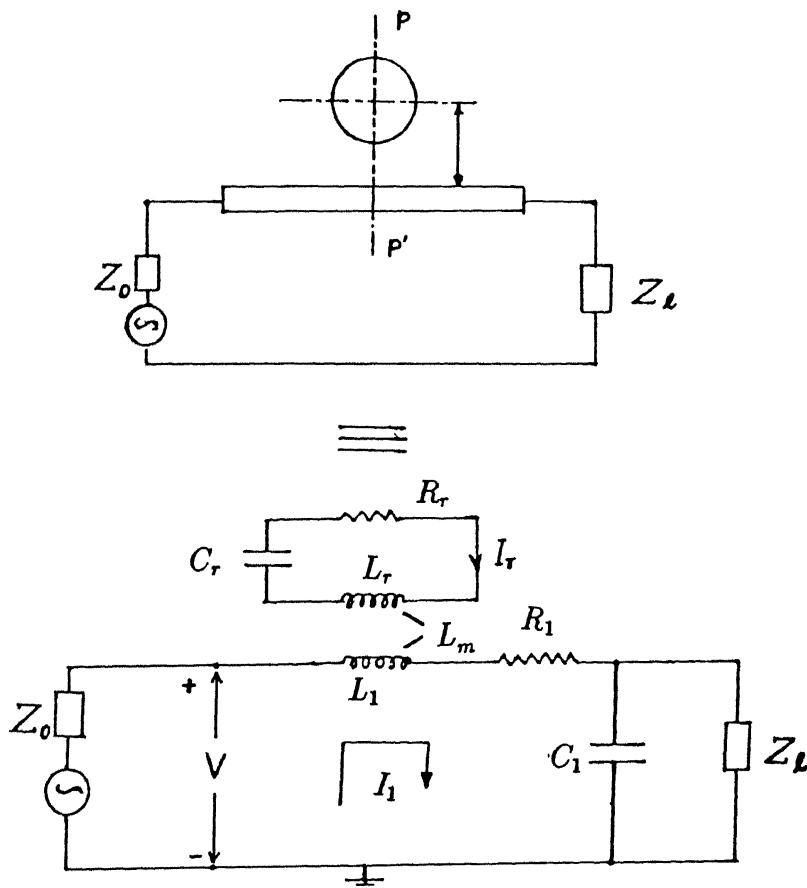


Fig. 5.3: Equivalent circuit representation of dielectric resonator coupled to a transmission line [32]

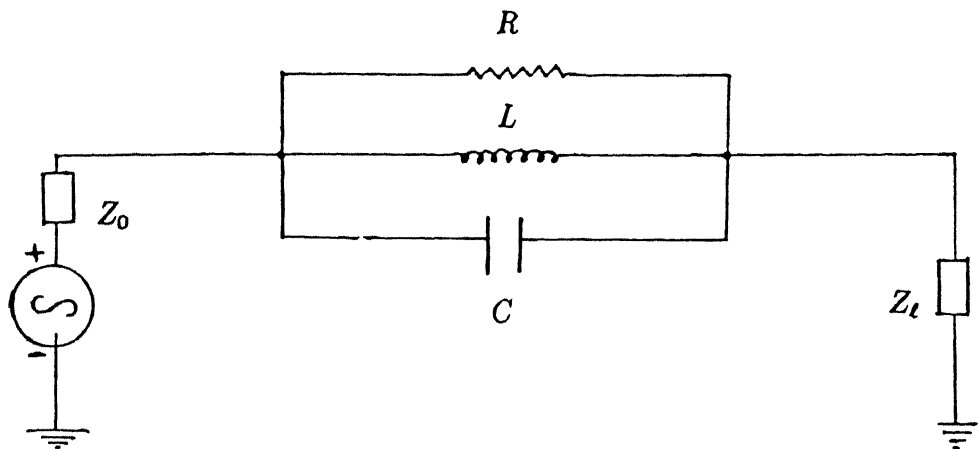


Fig. 5.4: Equivalent parallel tuned circuit [7]

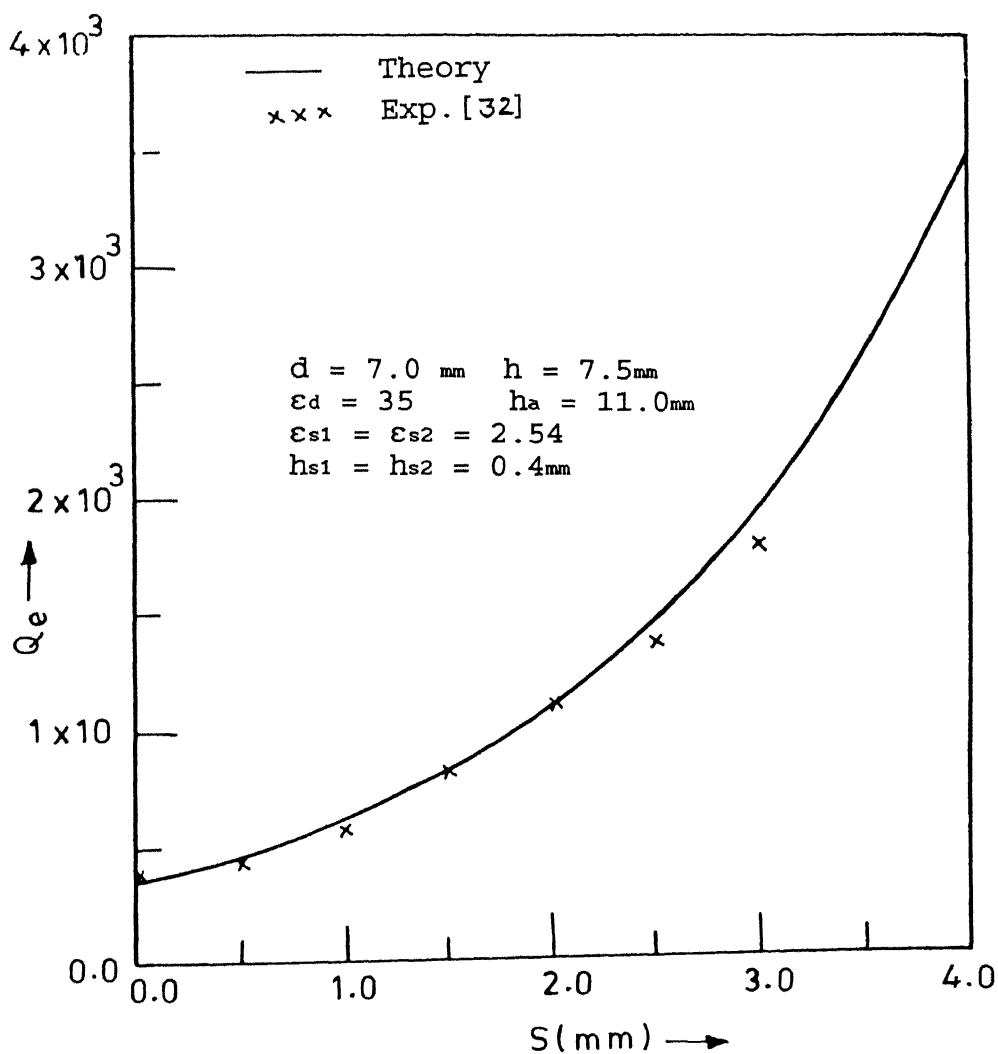


Fig. 5.5: Comparison of theoretical results with experimental data for microstrip environment

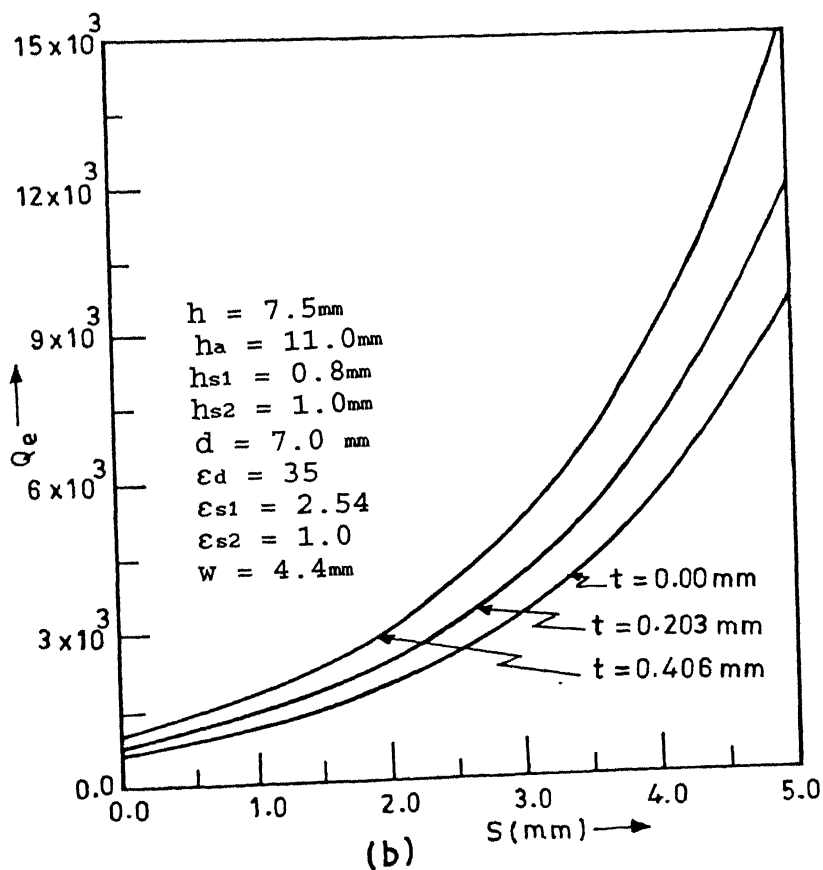
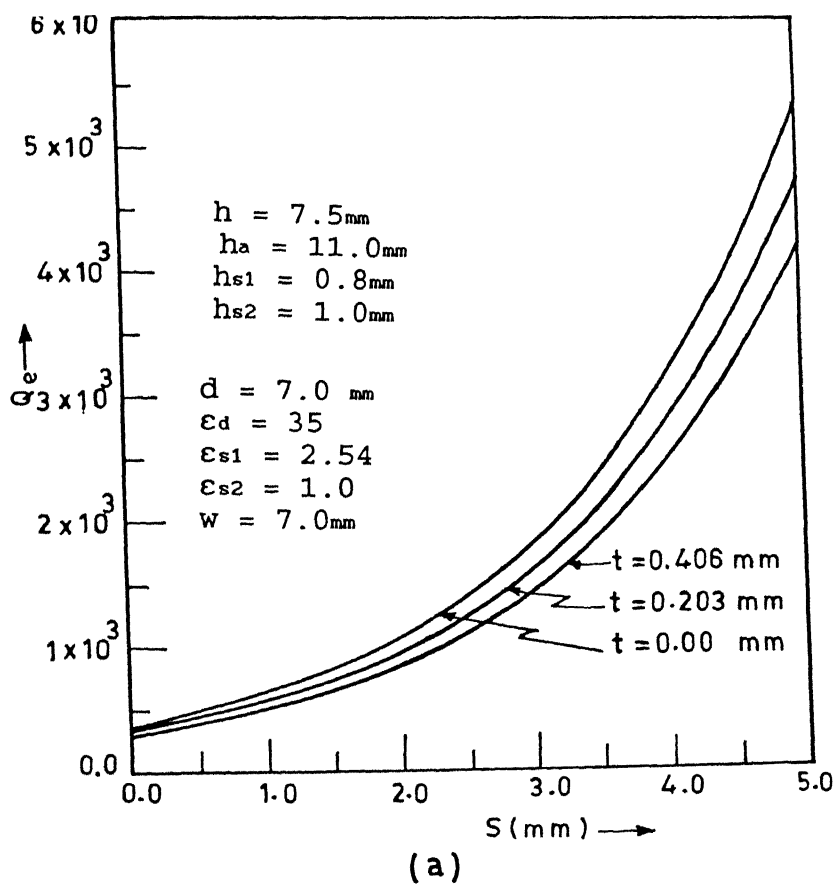


Fig. 5.6: Q_e 's variation as function of s for S-band (a) suspended stripline case. (b) inverted microstripline case

Chapter 6

CONCLUSION AND FUTURE DEVELOPMENTS

The dielectric resonator is studied in suspended substrate environment. The design parameters like resonant frequency, field configuration, energy distribution, coupling between two resonators and coupling between dielectric resonator with planar transmission lines are derived, in suspended substrate environment for millimeter wave applications. The main focus is on most commonly used $TE_{01\delta}$ mode of cylindrical resonator. The resonant frequency is calculated using an improved effective dielectric constant technique with well known dielectric waveguide model (DWM) method. Then the fields and the energy distribution in all the regions of the structure is obtained. Using a magnetic dipole model for DR, the magnetic coupling is studied between two identical cylindrical resonators, for three important configurations. Coupling between cylindrical resonator and two important transmission line configurations like suspended stripline and inverted microstripline with finite thickness conductor, is studied using, simple lumped element model for DR and the line.

Software is developed using above analysis, which can be used for CAD of microwave circuits like filters, oscillators, mixers etc. The results are generated for microstripline configuration as a special case of suspended substrate configuration, and are compared with experimental data available in the literature. This comparison validates the present analysis.

Future Developments

To get the full application of Suspended substrate environment, the hybrid mode analysis of dielectric resonator is required. Practical realization of the

microwave circuits like filters, mixers, oscillators, etc., using DR in suspended substrate environment is required to verify the configurations like off layered DRs and inverted microstripline with DR. The Theoretical results are very interesting for these cases, but due to non availability of the experimental data in literature for these configurations, we could not verify it.

For upper band in millimeter wave range, the size of DR become very small, this problem can be solved by using Whispering gallery mode resonance in cylindrical resonators which allows the use of oversized resonators.

Appendix A

Value Of Field Constants B₁S

$$B_1 = \frac{\beta_1 \cdot \tanh(\alpha_a h_a) \cdot \tan(\beta_1 h/2) - \alpha_a}{\beta_1 \cdot \tanh(\alpha_a h_a) + \alpha_a \cdot \tan(\beta_1 h/2)}$$

$$B_2 = \frac{[\cos(\beta_1 h/2) + B_1 \cdot \sin(\beta_1 h/2)]}{e^{-\alpha_a d_1} \sinh(\alpha_a h_a)}$$

$$B_3 = \frac{[\cos(\beta_1 h/2) - B_1 \cdot \sin(\beta_1 h/2)]}{[\cos(\beta_2 h/2) - B_4 \cdot \sin(\beta_2 h/2)]}$$

$$B_4 = \frac{\alpha_s - \beta_2 \cdot \tanh(\alpha_s h_{s2}) \cdot \tan(\beta_2 d_3)}{\beta_2 \cdot \tanh(\alpha_s h_{s2}) + \alpha_s \cdot \tan(\beta_2 d_3)}$$

$$B_5 = \frac{B_3 \cdot [\cos(\beta_2 d_3) - B_4 \cdot \sin(\beta_2 d_3)]}{e^{-\alpha_s d_2} \sinh(\alpha_s h_{s2})}$$

$$B_6 = B_2 \cdot B_7$$

$$B_7 = \frac{J_0(k_r d)}{K_0(k_a \cdot \bar{d})}$$

$$B_8 = B_3 \cdot B_7$$

$$B_9 = B_5 \cdot B_7$$

where $d_1 = h_a + h/2$, $d_2 = h_{s2} + d_3$, and $d_3 = h_{s1} + h/2$.

Appendix B

Expressions for A_{ijs} and t_{sameS}

A_{ij} Expressions:

$$A_{16} = \int_{-h/2}^{h/2} [\cos(\beta_1 z) + B_1 \sin(\beta_1 z)]^2 dz$$

$$A'_{16} = \int_{-h/2}^{h/2} [\sin(\beta_1 z) - B_1 \cos(\beta_1 z)]^2 dz$$

$$A_{18} = \int_{-h/2}^{h/2} \sinh\{\alpha_s(z+h_{s2}-h/2)\} [\cos(\beta_1 z) - B_1 \sin(\beta_1 z)] dz$$

$$A_{37} = \int_{-d_3}^{-h/2} [\cos(\beta_2 z) + B_4 \sin(\beta_2 z)]^2 dz$$

$$A'_{37} = \int_{-d_3}^{-h/2} [\sin(\beta_2 z) - B_4 \cos(\beta_2 z)]^2 dz$$

$$A_{37d} = \int_{h/2}^{h_{s1}+h/2} [\cos\{\beta_2(z-h_{s1}-h)\} + B_4 \sin\{\beta_2(z-h_{s1}-h)\}] \times [\cos(\beta_2 z) - B_4 \sin(\beta_2 z)] dz$$

t_{same} Expressions:

$$t_{\text{same}}(hs2, d2, \alpha_s) = \frac{[\sinh(2\alpha_s hs2) - 2\alpha_s hs2]}{e^{2\alpha_s d2} \cdot 4\alpha_s}$$

$$t_{\text{same}}(ha, d1, \alpha_a) = \frac{[\sinh(2\alpha_a ha) - 2\alpha_a ha]}{e^{2\alpha_a d1} \cdot 4\alpha_a}$$

$$t'_{\text{same}}(hs2, d2, \alpha_s) = \frac{[\sinh(2\alpha_s hs2) + 2\alpha_s hs2]}{e^{2\alpha_s d2} \cdot 4\alpha_s}$$

$$t'_{\text{same}}(ha, d1, \alpha_a) = \frac{[\sinh(2\alpha_a ha) + 2\alpha_a ha]}{e^{2\alpha_a d1} \cdot 4\alpha_a}$$

Appendix C

Integrals involving Bessel Functions

$$I_{jo} = \int_0^d r \cdot J_0^2(kr) \cdot dr$$

$$I_{ko} = \int_d^t r \cdot K_0^2(ka r) \cdot dr$$

$$I_{ej} = \int_0^d r \cdot J_1^2(kr) \cdot dr$$

$$I_{ek} = \int_d^t r \cdot K_1^2(ka r) \cdot dr$$

$$I_{jk} = \int_0^{2\pi} \int_0^d \frac{r \cdot [r + (2d+S) \cdot \sin(\phi)]}{r'} J_1(kr) K_1(ka \cdot r') dr d\phi$$

$$\text{where } r' = [r^2 + (2d+S)^2 + 2 \cdot r \cdot (2d+S) \cdot \sin(\phi)]^{1/2}$$

Appendix D

Evaluation of volume integral $\iiint \underline{E} \cdot \underline{J}$

The volume in above integration is the volume occupied by DR and its supporting substrate in which polarization current exists. For edge coupled case we are considering second medium as dielectric material with dielectric constant ϵ_{s2} and for suspended substrate case, this become air i.e. $\epsilon_{s2} = 1$. While for off layered dielectric resonators this medium is always air.

D.1 Edge Coupled case

Here the integral can be splitted in to different regions, and after substituting the value of polarization current from chapter 4 gives

$$\int_V \underline{E}^1 \cdot \underline{J}_p \, dv = j\omega_0 \epsilon_0 \{ (\epsilon_d - 1) \int_V (\underline{E}_6^1 \cdot \underline{E}_1^2) \, dv + (\epsilon_{s1} - 1) \int_V (\underline{E}_7^1 \cdot \underline{E}_3^2) \, dv + (\epsilon_{s2} - 1) \int_V (\underline{E}_8^1 \cdot \underline{E}_4^2) \, dv \} \quad (D.1)$$

where \underline{E}_j^i denotes the electric field due to i th resonator in its j th region.

The scalar product $(\underline{E}_j^i \cdot \underline{E}_l^k)$ may be obtained in terms of the x and y components of electric fields. For this purpose we are considering the geometry as shown in Fig. D.1, it is the bottom view of our structure (Fig. 4.2) which remains same for all three configurations. for off layered cases only we have to take care of z-coordinate transformation.

According this figure we find that

$$\underline{E}_j^i \cdot \underline{E}_l^k = E_j^i E_l^k (\cos\gamma \cdot \sin\phi + \sin\gamma \cdot \cos\phi) \quad (D.2)$$

where

$$\cos\gamma = (y + y_s)/r' \quad \sin\phi = y/r$$

$$\sin\gamma = x/r' \quad \cos\phi = x/r$$

$$\text{and } r' = \{r^2 + y_s^2 + 2y_s \cdot r \cdot \sin\phi\}^{1/2}$$

Appendix E

Derivation of Integral $\int \underline{H} \cdot d\underline{s}$

To incorporate the effect of thickness of the strip conductor, we have considered the induced emf on both sides surfaces of the conductor, and then taken average of it to get final expression of $\int \underline{H} \cdot d\underline{s}$, which is representing the induced emf on the conductor. On both sides of the conductor we will break the surface of integration s into parts according to the region number. The trick is same for both the cases i.e. suspended strip line and inverted microstripline. We are representing the surfaces as s_{top} , and s_{bottom} for top side plane of the strip and that towards the ground conductor, respectively.

For suspended stripline case, we can write

$$s_{top} = S5 + S6 \quad \text{and} \quad s_{bottom} = S7 + S8 \quad (E.1)$$

and, for inverted microstripline, we can write

$$s_{top} = S5 + S6 + S7 \quad \text{and} \quad s_{bottom} = S8 \quad (E.2)$$

After deciding the surface of integration, now we can consider the Integrand i.e. $\underline{H} \cdot d\underline{s}$. As we know that for $TE_{01\delta}$ mode we have H_r and H_z components of \underline{H} , but H_z component is normal to the surface vector so its dot product with the surface will be zero. Now only we have to consider H_r component. As shown in the Fig E.1 the $H_r \cdot \sin\phi$ component is again normal to the surface vector so by same region it also vanishes. Hence, we have finally the integrant w.r.t. the Fig.E.1, as follows,

$$(\underline{H} \cdot d\underline{s})_i = H_{r1} \cdot \cos\phi \, dx \, dz \quad (E.3)$$

where the subscript i denotes the region number in which the integration is to be performed.

From the geometry of Fig. E.1 we can write

$$\cos\phi = b / \{x^2 + b^2\}^{1/2} \quad \text{and} \quad r = \{x^2 + y^2\}^{1/2} \quad (E.4)$$

After substituting the value of $\cos\phi$ and that of the r in to

field expressions of H , we get the final expressions of integration in different regions. Then put these values into eqs. (E.1) and (E.2), for suspended stripline and inverted microstripline respectively.

Finally

$$\int \underline{H} \cdot d\underline{s} = [|\{ \int \underline{H} \cdot d\underline{s} \}_{stop}| + |\{ \int \underline{H} \cdot d\underline{s} \}_{Sbottom}|] / 2 \quad (E.5)$$

For both the cases,

$$\begin{aligned} \{ \int \underline{H} \cdot d\underline{s} \}_{S5} &= B6 \cdot \exp(-\alpha_a d_1) \sinh(\alpha_a h_a) \cdot I_h / k_a \\ \{ \int \underline{H} \cdot d\underline{s} \}_{S7} &= B8 [\cos(\beta_2 d_3) - \cos(\beta_2 h/2) \\ &\quad - B4 \{ \sin(\beta_2 d_3) - \sin(\beta_2 h/2) \}] I_h / k_a \end{aligned} \quad (E.6)$$

But for suspended stripline:

$$\begin{aligned} \{ \int \underline{H} \cdot d\underline{s} \}_{S8} &= - B9 \cdot \exp(-\alpha_s d_2) \sinh(\alpha_s h_{s2}) \cdot I_h / k_a \\ \{ \int \underline{H} \cdot d\underline{s} \}_{S6} &= B7 [\cos(\beta_1 h / \sqrt{2-t}) - \cos(\beta_1 h/2) \\ &\quad - B1 \{ \sin(\beta_1 h/2) + \sin(\beta_1 h / \sqrt{2-t}) \}] I_h / k_a \end{aligned} \quad (E.7)$$

and, for inverted microstripline:

$$\begin{aligned} \{ \int \underline{H} \cdot d\underline{s} \}_{S6} &= -2B1B7 \sin(\beta_1 h/2) I_h / k_a \\ \{ \int \underline{H} \cdot d\underline{s} \}_{S8} &= - B9 \cdot \exp(-\alpha_s d_2) \sinh(\alpha_s \overline{h_{s2}-t}) \cdot I_h / k_a \end{aligned} \quad (E.8)$$

In the above expressions, t is the thickness of the strip conductor. The coupling plane between DR and strip-conductor is at l_1 distance from feeding end and at l_2 distance from terminal load where the length of the line is (l_1+l_2) and width is w . This is shown in the Fig E.1. The integral I_h is as follows:

$$I_h = \int_{-1}^{1/2} K_1 \{ k_a (x^2 + b^2)^{1/2} \} \cdot b / \{ (x^2 + b^2)^{1/2} \} dx \quad (E.9)$$

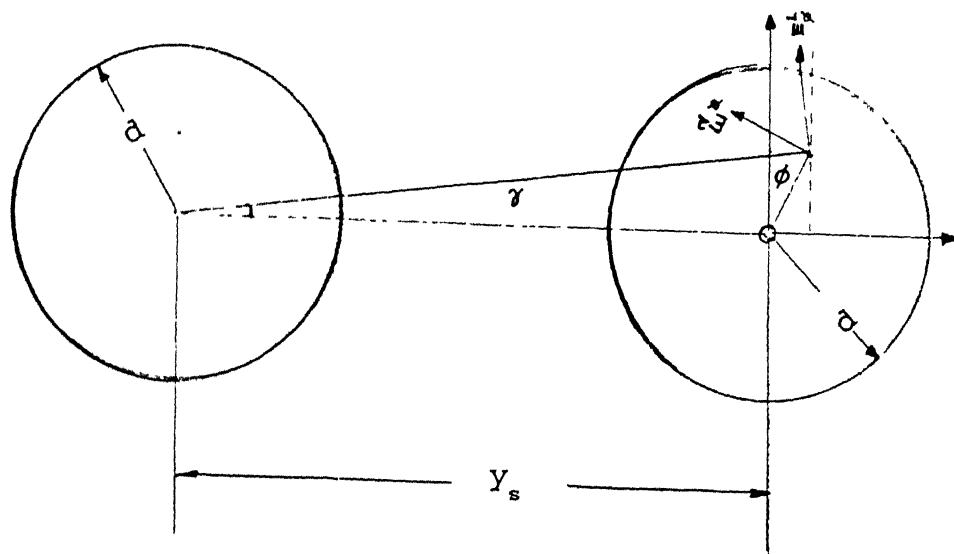


Fig. D.1: Bottom view of two directly coupled DRs

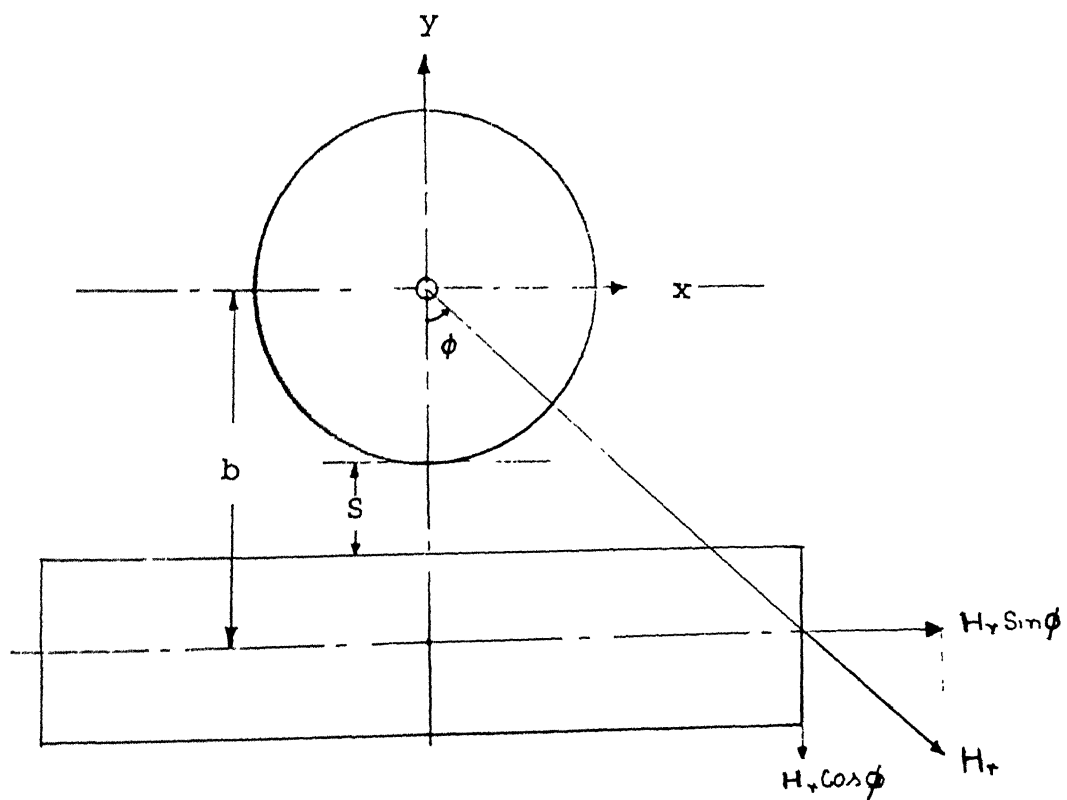


Fig. E.1: Evaluation of Integral $\underline{H} \cdot d\underline{s}$

REFERENCES

- [1] R.F. Harrington, *Time Harmonic Electromagnetic fields*, McGrawHill, New York, 1961.
- [2] R.E. Collin, *Field theory of guided waves*, McGrawHill, New York, 1960.
- [3] R.E. Collin, *Foundation for microwave engineering*, McGrawHill, New York, 1966
- [4] C.A. Balanis, *Advanced engineering electromagnetics*, John Wiley Sons, USA, 1989.
- [5] E.C. Jordan and K.G. Balmain, *Electromagnetic waves and radiation systems*, Prentice Hall, New Delhi, 1989.
- [6] F. Monaco, *Introduction to microwave technology*, Merill Publishing Company, USA, 1989.
- [7] D. Kajfez and P. Guillon, *Dielectric Resonators*, Artec House, Norwood MA, 1986.
- [8] K.J. Button, *Topics in millimeter wave technology*, Volume-1, Academic Press, Inc. (LONDON) Ltd., 1988.
- [9] K.C. Gupta, R. Garg, and I.J. Bahl, *Microstriplines and Slotlines*, Artec House, INC., Dedham, MA, 1979.
- [10] K.C. Gupta, R. Garg, and R. Chada, *Computer aided design of Microwave circuits*, Artec House, INC., Dedham, MA, 1981.

[11] T. Hopkins and C. Phillips, *Numerical Methods in Practice using the NAG library*, Addison-Wesley Publishing Company, Inc., 1988.

[12] Trans Tech inc., *Dielectric resonators : a designer's guide to microwave dielectric ceramics*, Oct.1990.

[13] K. Chang, *Handbook of Microwave and Optical Components*, Volume-1, Wildly Interscience Publication, 1989.

[14] S.B. Cohn, "Microwave band pass filters containing high-Q dielectric resonators," *IEEE Trans. Microwave Theory Tech.*, vol. MTT-16, pp. 218-227, 1968.

[15] T.D. Iveland, "Dielectric Resonator Filters for Application in Microwave Integrated Circuits," *IEEE Trans. Microwave Theory Tech.*, Vol. MTT-19, pp. 643-652, July 1971.

[16] N. Hoshino, Y. Konishi and Y. Utsami, "Resonant frequency of a TE_{01δ} dielectric resonators," *IEEE Trans. Microwave Theory Tech.* vol. MTT-24, pp. 112-114, Feb. 1976.

[17] T. Itoh and R.S. Rudokas, "New Method for Computing the Resonant Frequencies of Dielectric Resonators," *IEEE Trans. Microwave Theory Tech.*, Vol. MTT-25, pp. 52-54, Jan. 1977.

[18] U.S. Hong and R.H. Jansen, "Numerical analysis of shielded dielectric resonator including substrate, support disc and tuning post," *Electronic Lett.*, vol. 18, pp. 1000-1002, Non. 1982.

[19] D. Maystre, P. Vincent and J.C. Mage, "Theoretical and Experimental Study of the Resonant Frequency of a Cylindrical Dielectric Resonator," *IEEE Trans. Microwave Theory Tech.*, Vol. MTT-31, pp. 844-848, Oct. 1983.

[20] R.K. Mongia, ''Resonant Frequency of Cylindrical Dielectric Resonator Placed in an MIC Environment,'' *IEEE Trans. Microwave Theory Tech.*, Vol. MTT-38, pp. 802-805, June 1990.

[21] M.W. Pospieszalski, ''Cylindrical Dielectric Resonators and Their Application in TEM Line Microwave Circuits,'' *IEEE Trans. Microwave Theory Tech.*, Vol. MTT-27, pp. 233-238, March 1979.

[22] M. Jaworski and M.W. Pospieszalski, ''An accurate solution of dielectric resonator problem,'' *IEEE Trans. Microwave Theory Tech.*, vol. MTT-27, pp. 639-644, July 1979.

[23] J.K. Plourde and Chung-Liren, ''Application of Dielectric Resonators in Microwave Components,'' *Microwave Theory Tech.*, Vol. MTT-29, pp. 754-770, August 1981.

[24] D. Kajfez, A.W. Glisson and J. James, ''Evaluation of modes in dielectric resonators using a surface integral equation formulation,'' *IEEE Trans. Microwave Theory Tech.*, vol. MTT-31, pp. 1023-1029, Dec. 1983.

[25] H. Shigesawa, M. Tsuji and K. Takiyama, ''Analytical and experimental investigation on several resonant modes in open dielectric resonators,'' *IEEE Trans. Microwave Theory Tech.*, vol. MTT-32, pp. 628-633, June 1984.

[26] T. Higashi and T. Makino, ''Resonant frequency stability of the dielectric resonator on a dielectric substrate,'' *IEEE Trans. Microwave Theory Tech.*, vol. MTT-29, pp. 1048-1052, Oct. 1981.

[27] C. Tsironis and V. Pauker, ''Temperature stability of GaAs MESFET oscillators using dielectric resonators,'' *IEEE Trans. Microwave Theory Tech.*, vol. MTT-31, pp. 312-314, March 1983.

[28] Y. Kobayashi and M. Katoh, "Microwave Measurement of dielectric properties of low-loss materials by the dielectric rod resonator method," *IEEE Trans. Microwave Theory Tech.*, vol. MTT-33, pp. 586-592, July 1985.

[29] L. Pettersson, "On the Theory of Coupling Between Finite Dielectric Resonators," *Microwave Theory Tech.*, Vol. MTT-24, pp. 615-619, Sept. 1976.

[30] P. Skalicky, "Direct Coupling Between Dielectric Resonators," *Electronic Lett.* Vol. 18, pp. 332-334, April 1982.

[31] Y. Komatsu and Y. Murakami, "Coupling Coefficient Between Microstripline and Dielectric Resonator," *Microwave Theory Tech.*, Vol. MTT-31, pp. 34-40, Jan. 1983.

[32] P. Guillon, B. Byzery and M. Chaubet, "Coupling Parameters Between a Dielectric Resonator and a Microstripline," *Microwave Theory Tech.*, Vol. MTT-33, pp. 222-226, March 1985.

[33] K.A. Zaki and C. Chen, "New Results in Dielectric-Loaded Resonators," *Microwave Theory Tech.*, Vol. MTT-34, pp. 815-824, July 1986.

[34] D. Kajfez, "Indefinite Integrals Useful in the Analysis of Cylindrical Dielectric Resonators," *Microwave Theory Tech.*, Vol. MTT-35, pp. 873-874, Sept. 1987.

[35] A.E. Centeno and G.B. Morgan, "Design of millimeter wave dielectric resonators for integrated circuits," *IEE Proc. (H)*, Vol.139, pp. 307-308, June 1992.

[36] M. Stiplitz, "Frequency Tuning of Rutile Resonators," *In. Proc. IEEE*, Vol.54, pp. 413-414, March 1966.

[37] S.W. Chen, K.A. Zaki and R. West, "Tunable Temperature Compensated Dielectric Resonators and Filters," *Microwave Theory Tech.*, Vol. MTT-38, pp. 1046-1049, August 1990.

[38] K. Warkino, T. Nishikawa and Y. Ishikawa, "Miniaturization Technologies of Dielectric Resonator Filters for Mobile Communications," *Microwave Theory Tech.*, Vol. MTT-42, pp. 1295-1300, July 1994.

[39] G. Macchiarella and G.B. Stracca, "An Accurate Design Approach for TM Mode Dielectric Resonator Filters in Circular Waveguide Below Cutoff," *Microwave Theory Tech.*, Vol. MTT-42, pp. 1321-1329, July 1994.

[40] R.K. Mongia, C.L. Larose, S.R. Mishra and P. Bhartia, "Accurate Measurement of Q-Factors of Isolated Dielectric Resonators," *Microwave Theory Tech.*, Vol. MTT-42, pp. 1463-1467, August 1994.

[41] B. Sauviac, P. Guillot and H. Baudrand, "Rigorous Analysis of Shielded Cylindrical Dielectric Resonators by Dyadic Green's Functions," *Microwave Theory Tech.*, Vol. MTT-42, pp. , August 1994.

[42] D. Kajfez and J. Guo, "Precision measurement of coupling between microstrip and TE₀₁ mode dielectric resonator," *Electronic Lett.* Vol. 30, pp. 1771-1772, Oct.1994.

[43] A. Jain, "Studies on Dielectric Resonator and design of a band pass filter in MIC environment," MTech. Thesis, Dept. of Electrical Engg., IIT-Kanpur, November-1993.